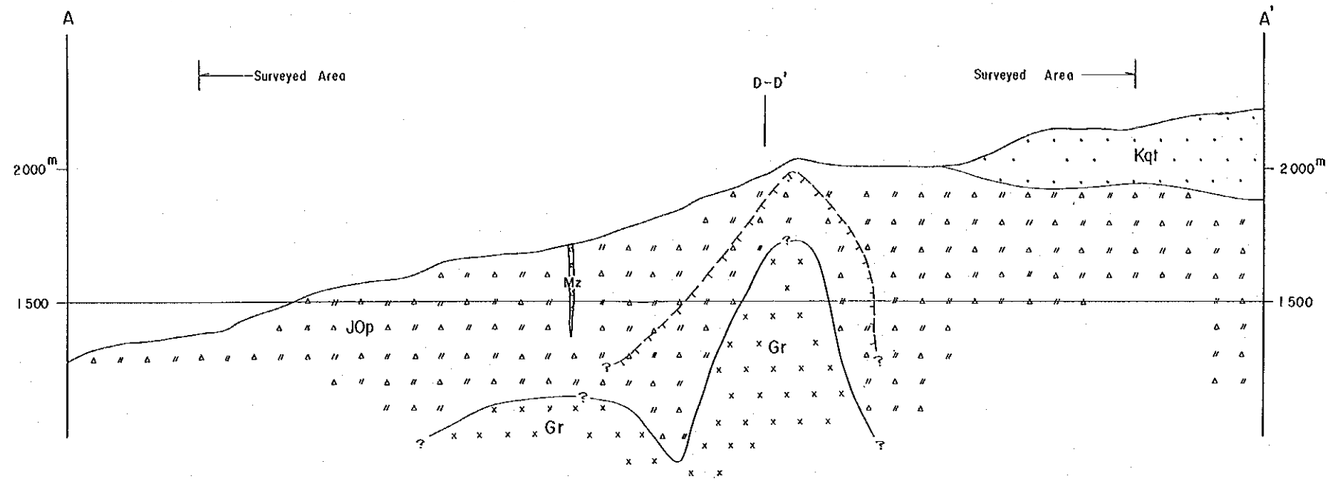
A
A'
Surveyed Area
Surveyed Area
D-D'
2000 m
1500
2000 m
1500
Kqt
Mz
JOp
Gr
Gr

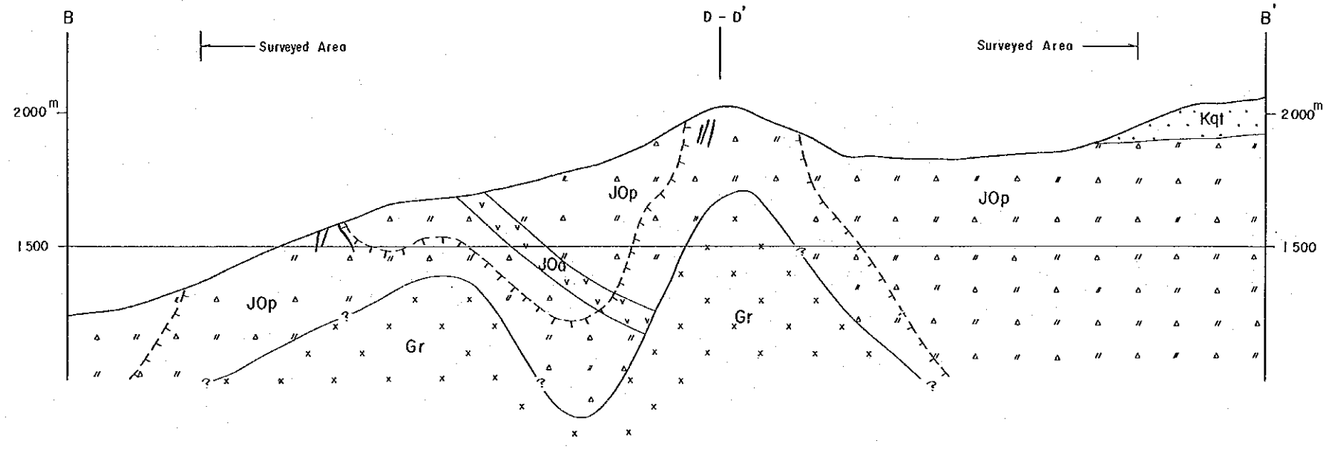
B
B'
Surveyed Area
Surveyed Area
D - D'
2000 m
1500
2000 m
1500
Kqt
JOp
JOp
JOa
JOp
Gr
Gr
JOp

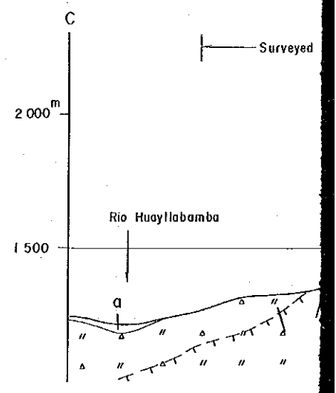
C
Surveyed
2 000 m
Rio Huayllabamba
1 500
a

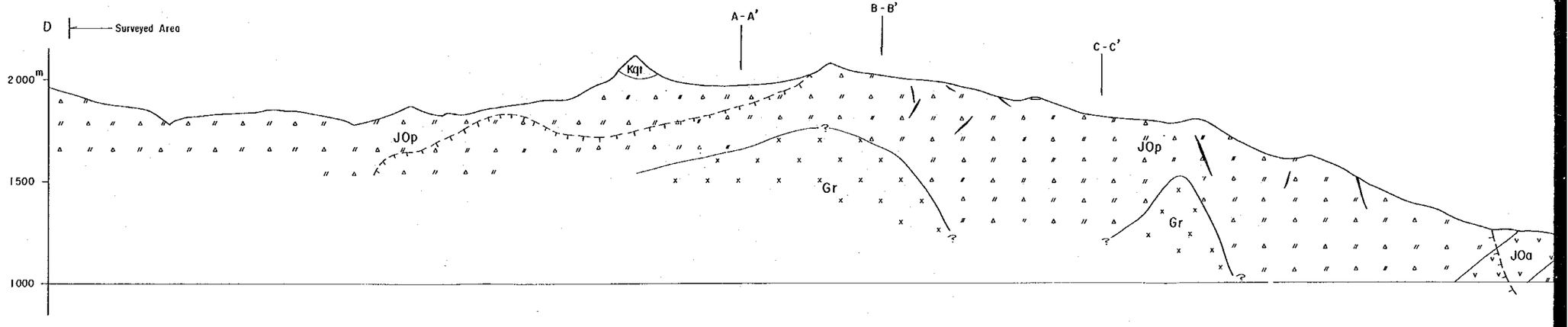
D
Surveyed Area
A - A'
B - B'
C - C'
2000 m
1500
1000
Kqt
JOp
Gr
JOp
Gr
JOp
JOa

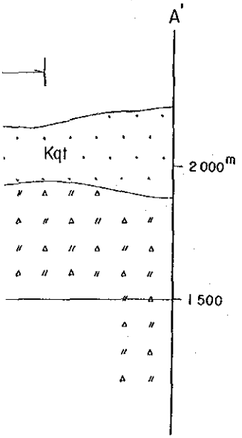

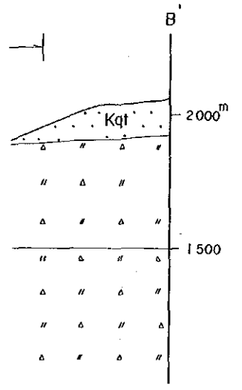

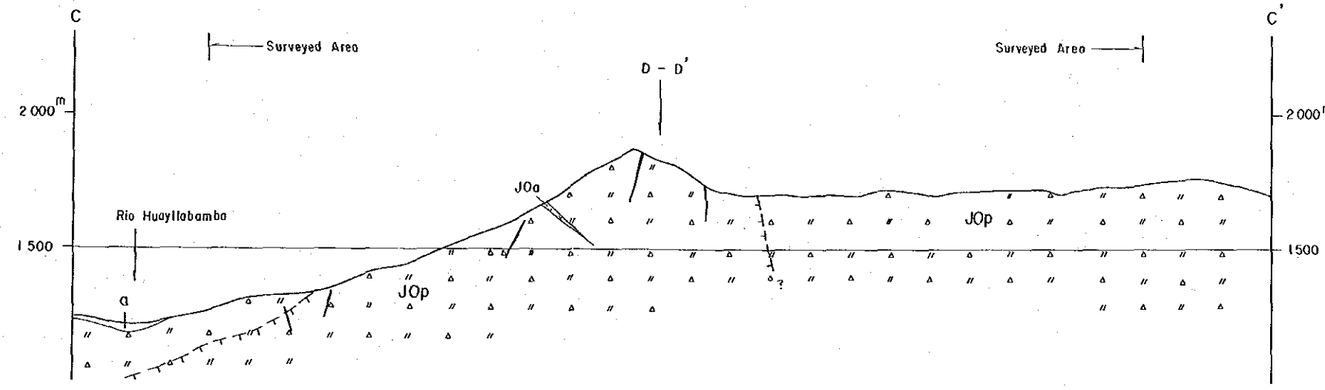

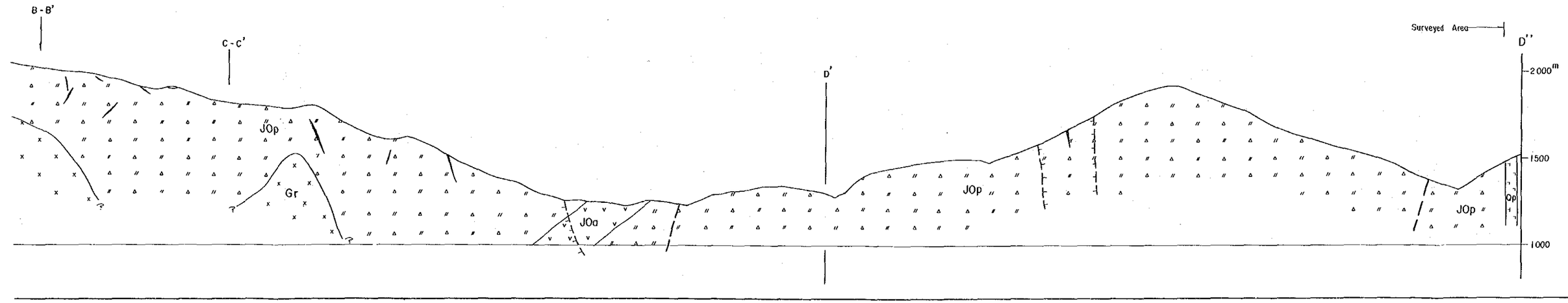

Quaternary

Cretaceous

Jurassic

Triassic

Fig

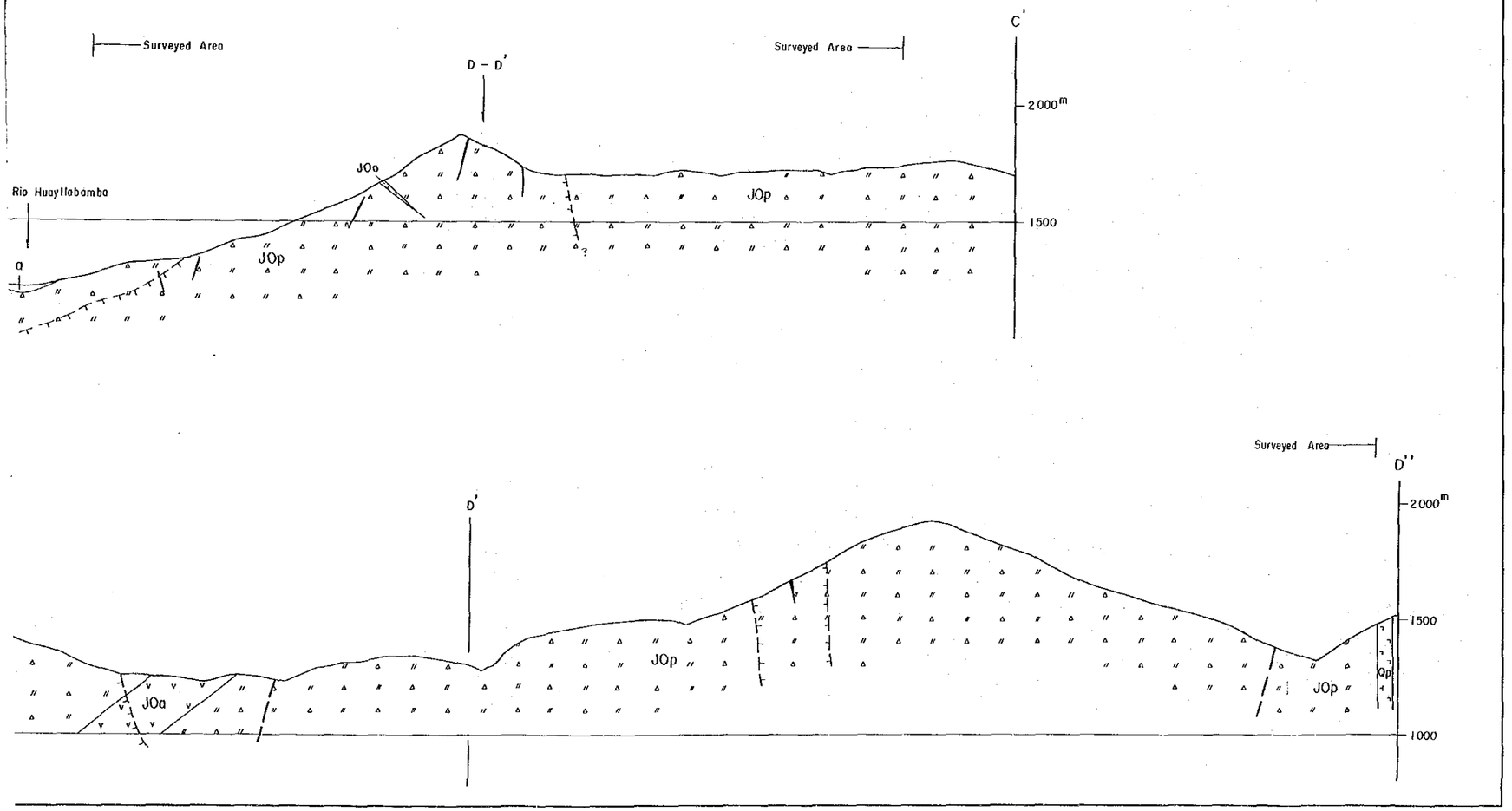

THE MINERAL EXPLORATION

IN

THE PACHAPIRIANA AREA, REPUBLIC OF PERU

(PHASE II)

GEOLOGICAL PROFILES OF THE CHONTALI AREA

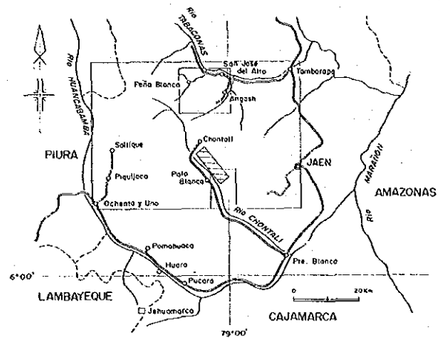

JAPAN INTERNATIONAL COOPERATION AGENCY

METAL MINING AGENCY OF JAPAN

FEBRUARY 1990

Prepared by MINDECO

0 500 1000m

LEGEND

Quaternary	Alluvium		Q	Gravel, Sand
Cretaceous	Goyllo-risquizgo	GP.	Kgt	Quartzite
Jurassic	Oyotun Vol.		JOq	Sandstone, Quartzite, Shale
			JOp	Tuff, Lapilli Tuff, Tuff Breccia
Triassic			JOa	Andesite
Intrusives			Mz	Monzonite
			Qp	Quartz Porphyry
Alteration				Silicified Zone or Silified Zone with Argillization
Others				Quartz Vein
				Fault
				Bedding

Fig. II-2 (2) Geological Profiles of the Chontali Area

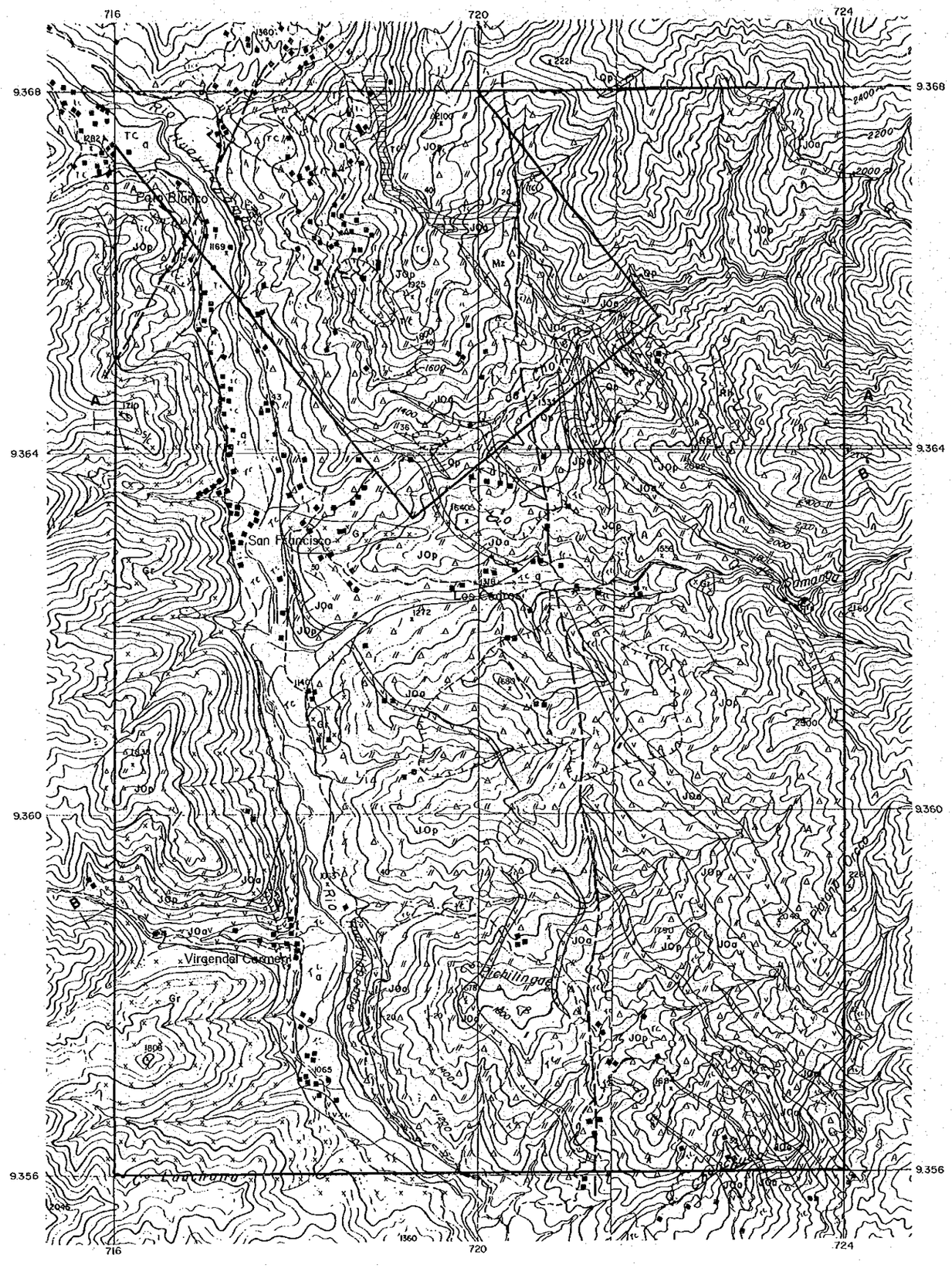

THE MINERAL EXPLORATION
IN
THE PACHAPIRIANA AREA, REPUBLIC OF PERU
(PHASE II)

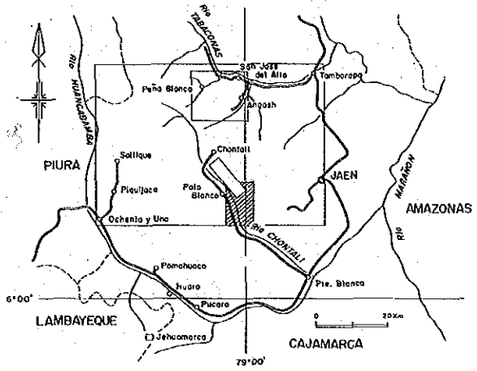

JAPAN INTERNATIONAL COOPERATION AGENCY
METAL MINING AGENCY OF JAPAN
FEBRUARY 1990
Prepared by MINDECO

0 2.5Km

LEGEND

Quaternary	Alluvium		Qa	
Jurassic ~ Triassic	Oyotun vol.		JOq	Sandstone, Quartzite, Shale
			JOp	Tuff, Lapilli Tuff, Tuff Breccia
			JOa	Andesite
Intrusives			Rh	Rhyolite
			Qp	Quartz Porphyry
			Mz	Monzonite
			Gr	Granodiorite, Granite
Alteration				Silicified Zone or Silicified Zone with Argillization
Others				Quartz Vein
				Bedding
				Fault

Fig. II-3 (1) Geological Map of the Chontali South Area

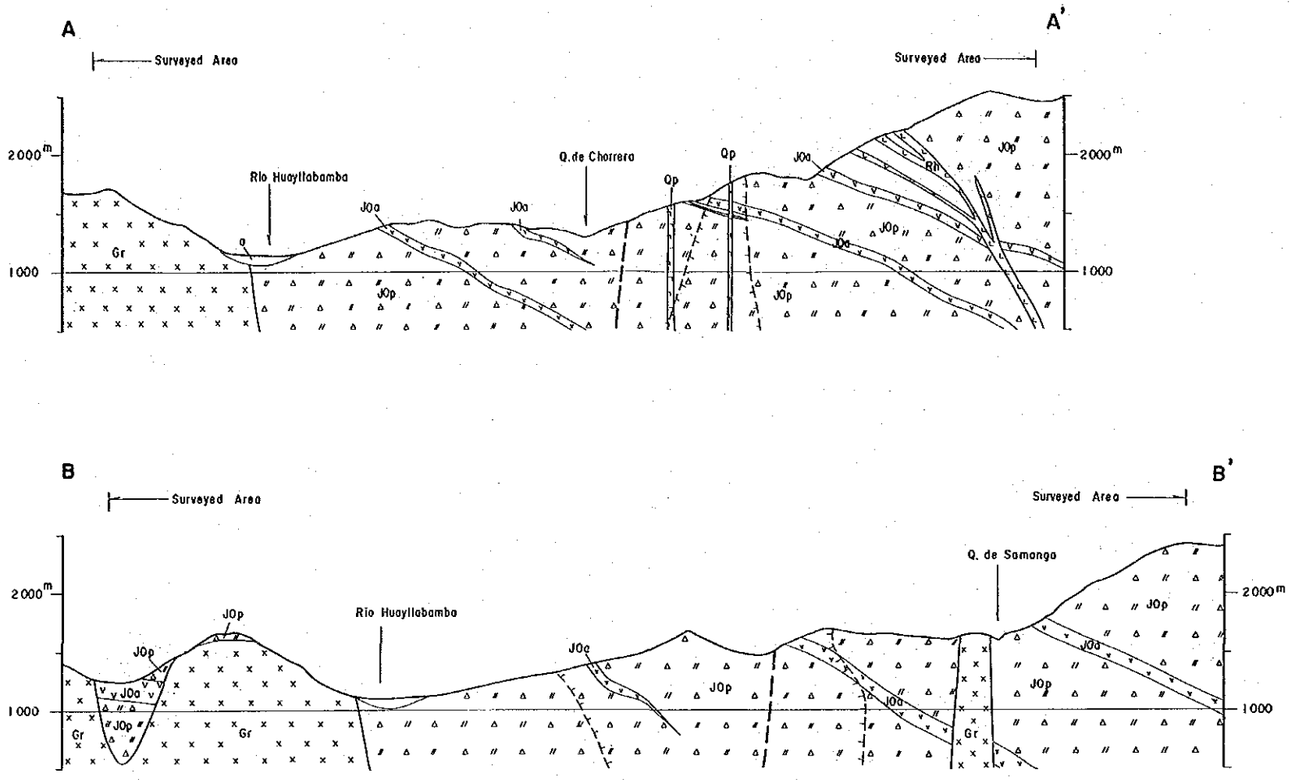

THE MINERAL EXPLORATION
IN
THE PACHAPIRIANA AREA, REPUBLIC OF PERU
(PHASE II)

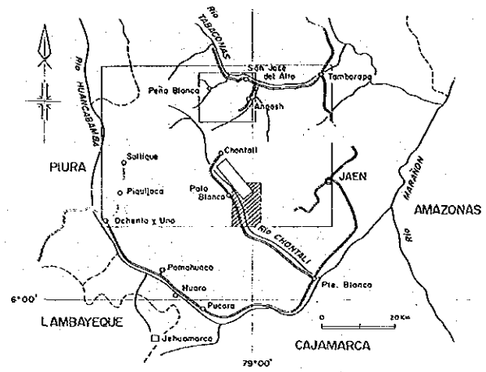

JAPAN INTERNATIONAL COOPERATION AGENCY
METAL MINING AGENCY OF JAPAN
FEBRUARY 1990
Prepared by MINDECO

0 2.5Km

LEGEND

Quaternary	Alluvium		a
Jurassic ⟆ Triassic	Oyotun vol.	JOq	Sandstone, Quartzite, Shale
		JOp	Tuff, Lapilli Tuff, Tuff Breccia
		JOa	Andesite
Intrusives		Rh	Rhyolite
		Qp	Quartz Porphyry
		Mz	Monzonite
		Gr	Granodiorite, Granite
Alteration			Silicified Zone or Silicified Zone with Argillization
Others			Quartz Vein
			Fault

Fig. II-3 (2) Geological Profiles of the Chontali South Area

A'

B'

C'

D

JOp

Kqt

Vista Alegre

Cumbara

Mz

Cruz Pampa

JOa

Hualaton

Tabocal

Los Laureles

Rio Huayllabamba

Los Piños

Palo Blanco

712

716

A

B

C

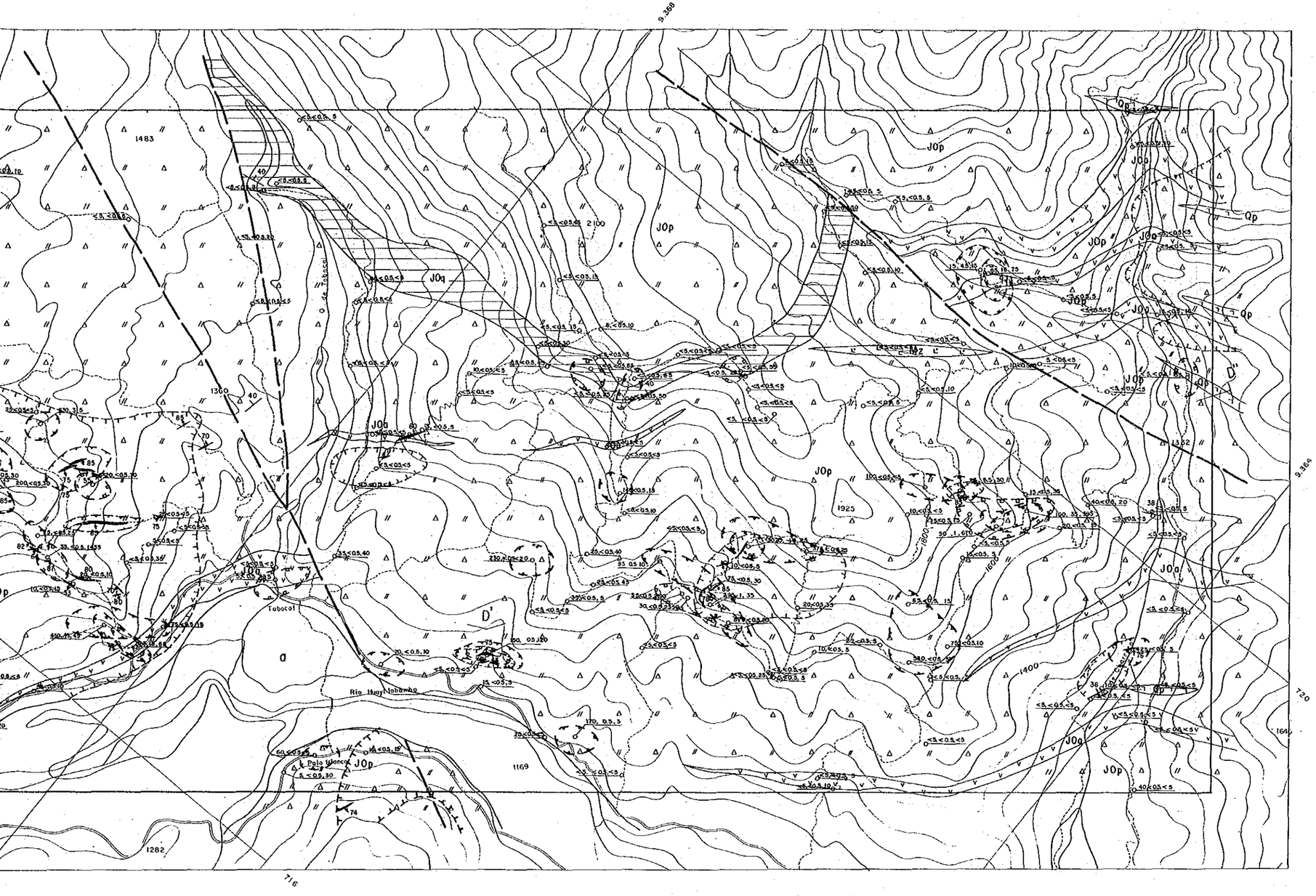

THE MINERAL EXPLORATION
IN
THE PACHAPIRIANA AREA, REPUBLIC OF PERU
(PHASE II)

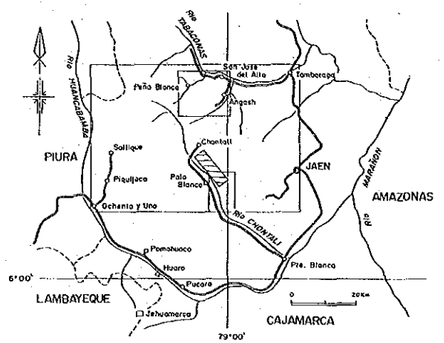

JAPAN INTERNATIONAL COOPERATION AGENCY
METAL MINING AGENCY OF JAPAN
FEBRUARY 1990
Prepared by MINDECO

0 500 1000m

LEGEND

Geochemical Anomaly

Au ≧ 50ppb
Ag ≧ 0.5ppm
Pb ≧ 50ppm

Quaternary	Alluvium		a	Gravel, Sand
Cretaceous	Goyllarisquizga GP.		Kgt	Quartzite
Jurassic	Oyotun Vol.		JOq	Sandstone, Quartzite, Shale
			JOp	Tuff, Lapilli Tuff, Tuff Breccia
Triassic			JOa	Andesite
Intrusives			Mz	Monzonite
			Qp	Quartz Porphyry
Alteration				Silicified and / or Argillized Zone
Others				Quartz Vein
				Fault
				Bedding

Fig. II-4(1) Distribution of Geochemical Anomaly in the Chontali Area
(Au,Ag ang Pb)

A' B' C'

D

JOp

Kql

Mz

Vista Alegre

Huatatón

Cumbara

Los Lourdes

Cruz Pampa

Tobacal

Rio Huayllo bambo

Rio Huayl Jobamba

Pata Blanca

Los Piños

1830

1708

1483

1360

1800

1600

1400

1282

2200

2000

2070

9.372

712

716

THE MINERAL EXPLORATION
IN
THE PACHAPIRIANA AREA, REPUBLIC OF PERU
(PHASE II)

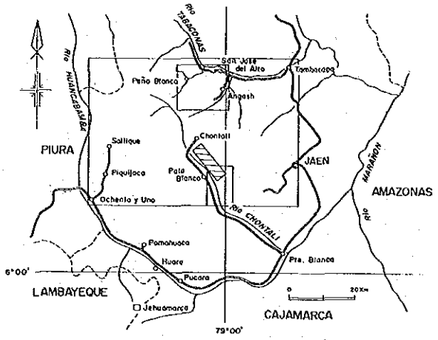

JAPAN INTERNATIONAL COOPERATION AGENCY
METAL MINING AGENCY OF JAPAN
FEBRUARY 1990
Prepared by MINDECO

0 500 1,000m

LEGEND

Geochemical Anomaly

Zn ≧ 100ppm
Cu ≧ 90 ppm
Mo ≧ 5 ppm

Quaternary	Alluvium	a	Gravel, Sand
Cretaceous	Goyllarisquizga GP.	Kgl	Quartzite
Jurassic	Oyotun Vol.	JOq	Sandstone, Quartzite, Shale
Triassic	Oyotun Vol.	JOp	Tuff, Lapilli Tuff, Tuff .Brec
	Oyotun Vol.	JOa	Andesite
Intrusives		Mz	Monzonite
		Qp	Quartz Porphyry
Alteration			Silicified and / or Argillized Zone
Others			Quartz Vein
			Fault
			Bedding

Fig. II-4(2) Distribution of Geochemical Anomaly in the Chontali Area
(Zn,Cu and Mo)

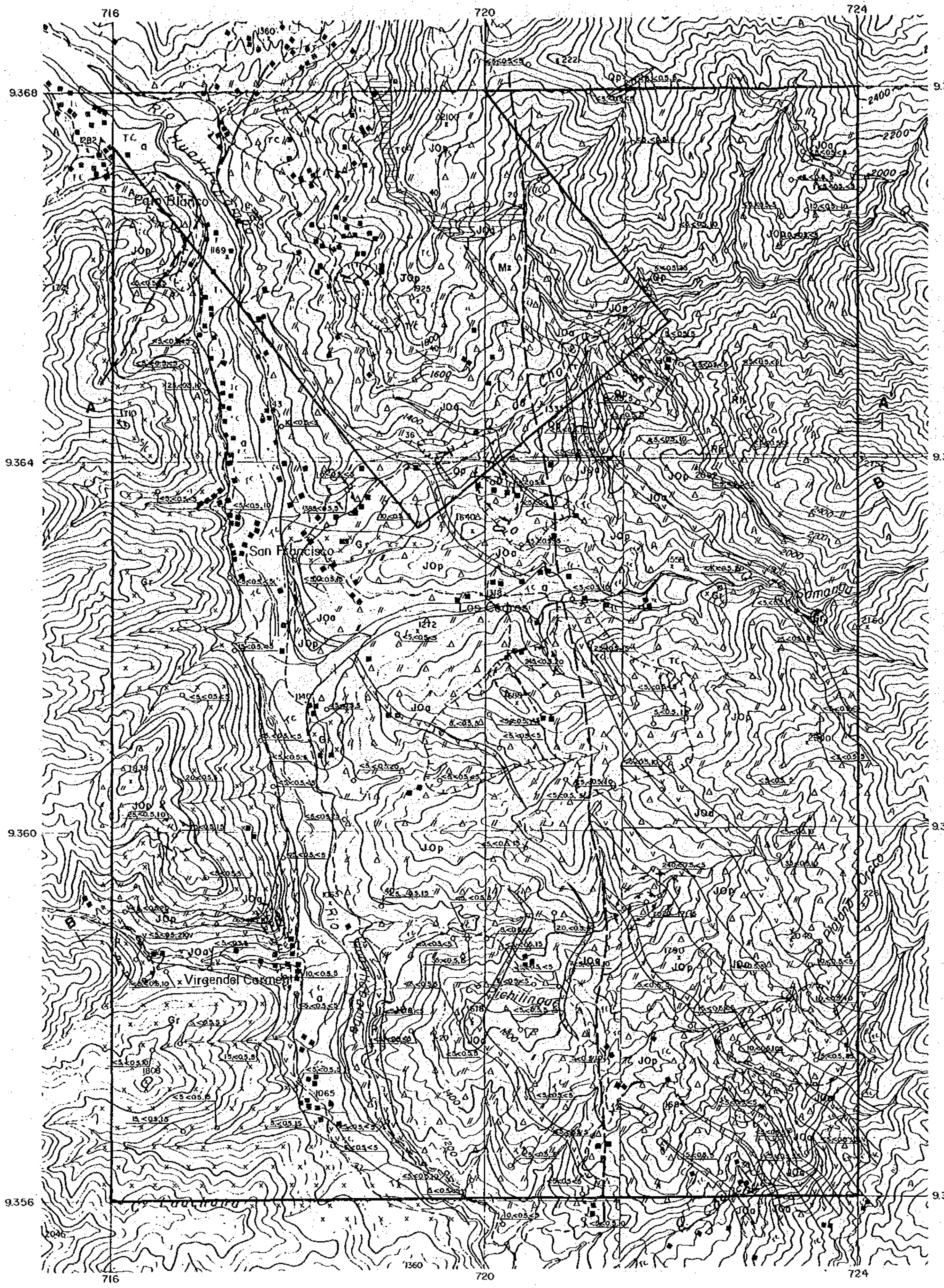

THE MINERAL EXPLORATION
IN
THE PACHAPIRIANA AREA, REPUBLIC OF PERU
(PHASE II)

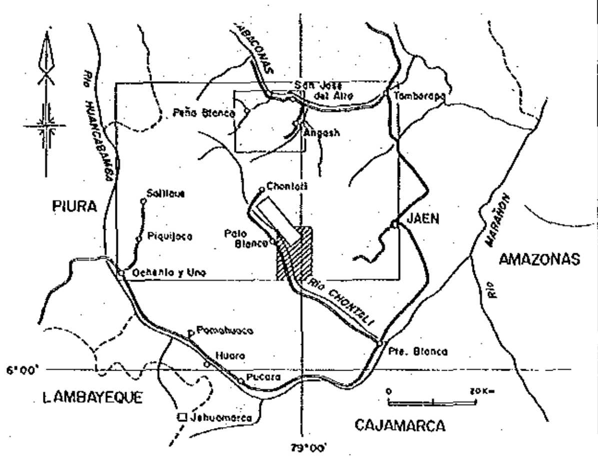

JAPAN INTERNATIONAL COOPERATION AGENCY
METAL MINING AGENCY OF JAPAN
FEBRUARY 1990
Prepared by MINDECO

0 2.5Km

LEGEND

Geochemical Anomaly
- Au ≧ 50 ppb
- Ag ≧ 05 ppm
- Pb ≧ 32 ppm

Alluvium — a

Oyolun vol.
- JOq — Sandstone, Quartzite, Shale
- JOp — Tuff, Lapilli Tuff, Tuff Breccia
- JOa — Andesite

Intrusives
- Rh — Rhyolite
- Qp — Quartz Porphyry
- Mz — Monzonite
- Gr — Granodiorite, Granite

Alteration — Silicified and / or Argillized zone

Others
- Quartz Vein
- Bedding
- Fault

Fig. II -5(1) Distribution of Geochemical Anomaly in the Chontali South Area (Au,Ag and Pb)

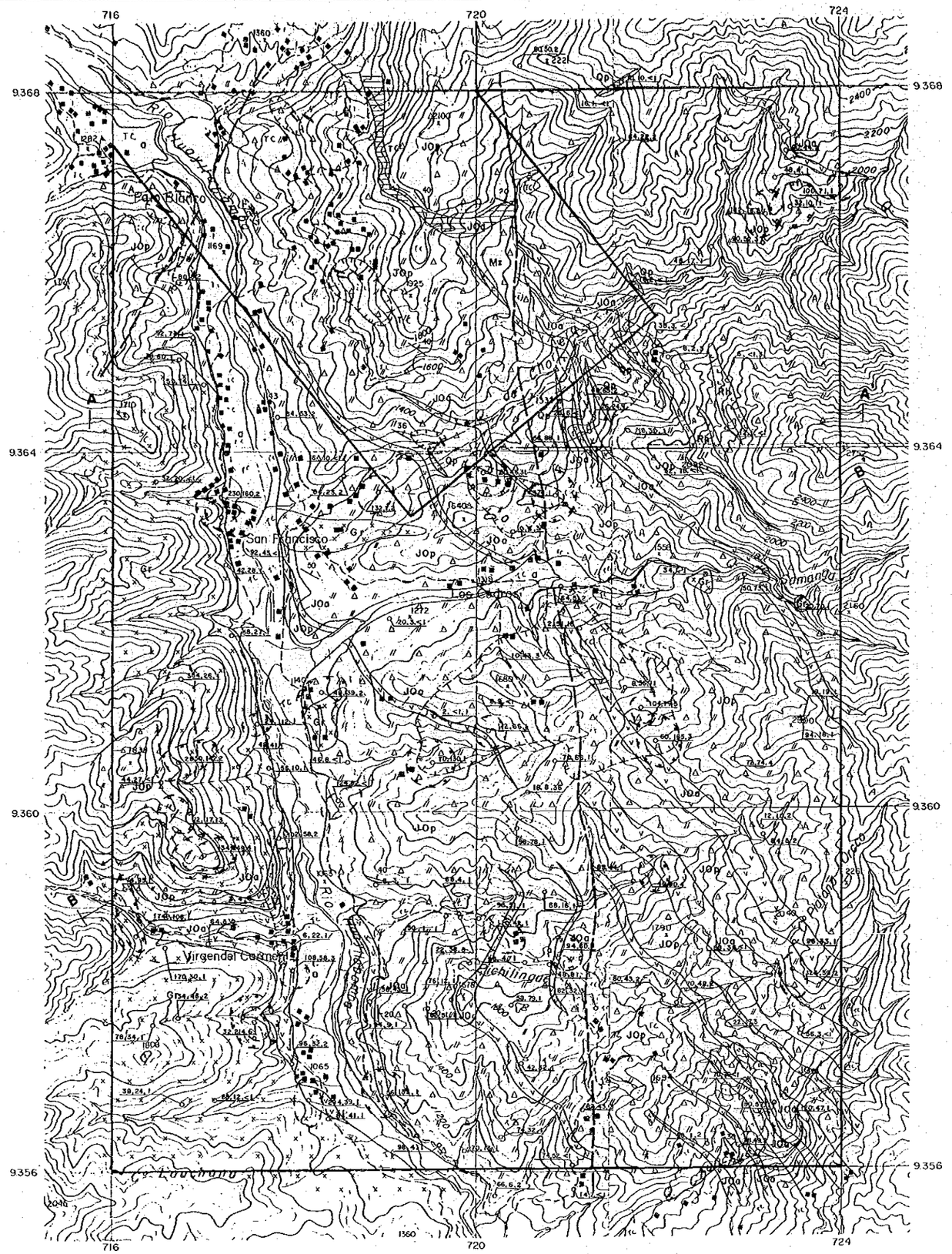

THE MINERAL EXPLORATION

IN

THE PACHAPIRIANA AREA, REPUBLIC OF PERU

(PHASE II)

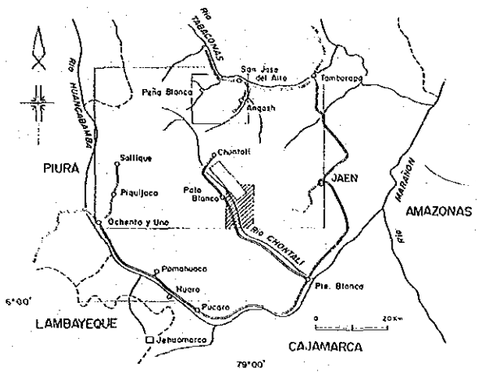

JAPAN INTERNATIONAL COOPERATION AGENCY

METAL MINING AGENCY OF JAPAN

FEBRUARY 1990

Prepared by MINDECO

0 2.5Km

LEGEND

Geochemical Anomaly

Zn ≧ 100ppm

Cu ≧ 90 ppm

Mo ≧ 5 ppm

Alluvium: Q

Oyotun vol.: JOq Sandstone, Quartzite, Shale; JOp Tuff, Lapilli Tuff, Tuff Breccia; JOa Andesite

Intrusives: Rh Rhyolite; Op Quartz Porphyry; Mz Monzonite; Gr Granodiorite, Granite

Alteration: Silicified and / or Argillized zone

Others: Quartz Vein; Bedding; Fault

Fig. II-5(2) Distribution of Geochemical Anomaly in the Chontali South Area (Zn,Cu and Mo)

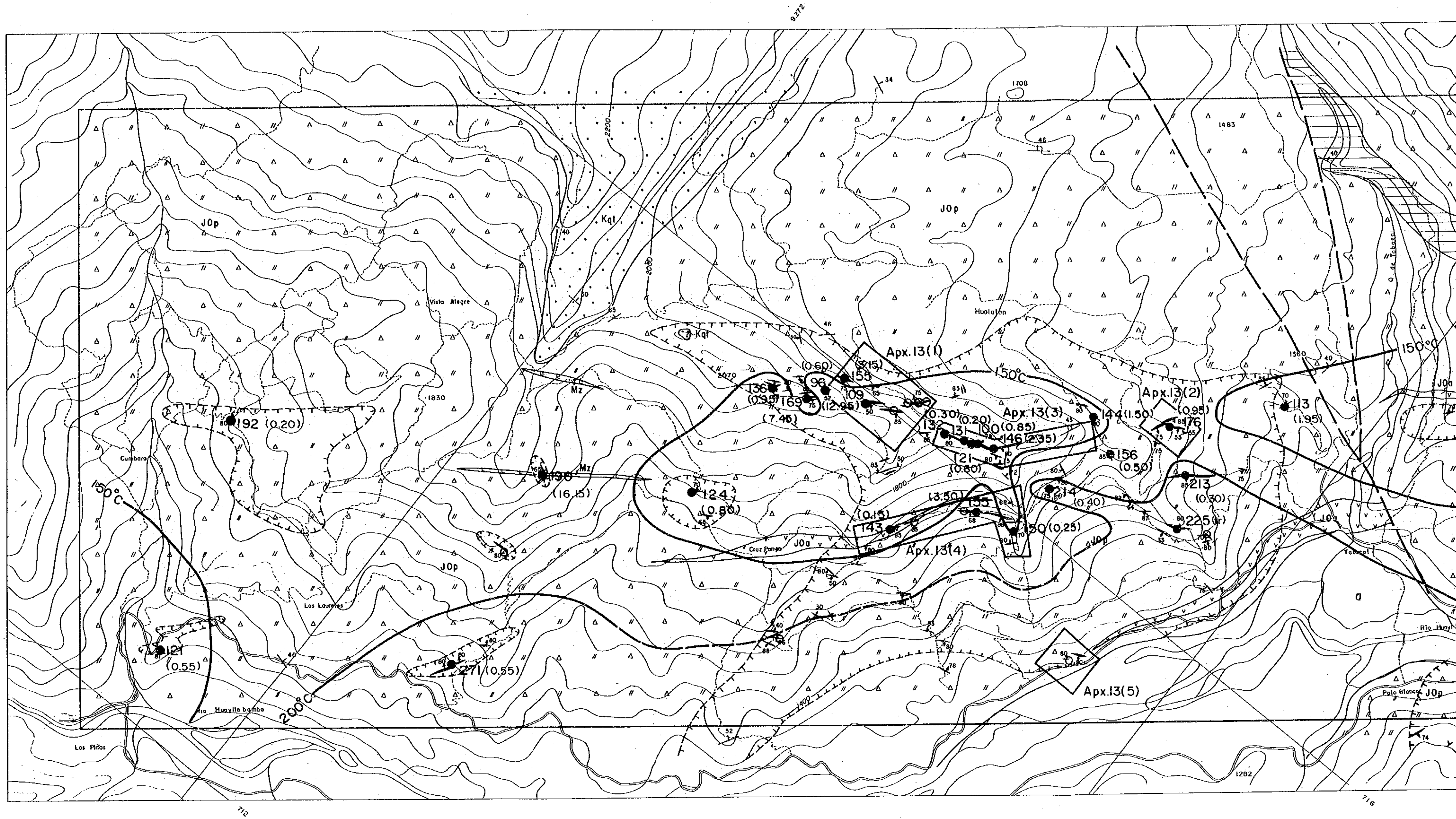

Apx.13(1)
Apx.13(2)
Apx.13(3)
Apx.13(4)
Apx.13(5)
150°C
200°C
J0p
J0a
Kql
Mz
Vista Alegre
Hualatan
Cumbaro
Los Laureles
Cruz Pampa
Tabacal
Los Piños
Rio Huayllabamba
Palo Blanco
192 (0.20)
190 (16.15)
124 (0.80)
121 (0.55)
271 (0.55)
136 (0.35)
169
96
155
109 (12.95)
(7.45)
(0.60)
144 (1.50)
156 (0.50)
146 (2.35)
131
132
121 (0.60)
143
135
150 (0.25)
213 (0.30)
225 (tr)
176 (0.95)
113 (1.95)
712
716
9372
1708
1483
1282

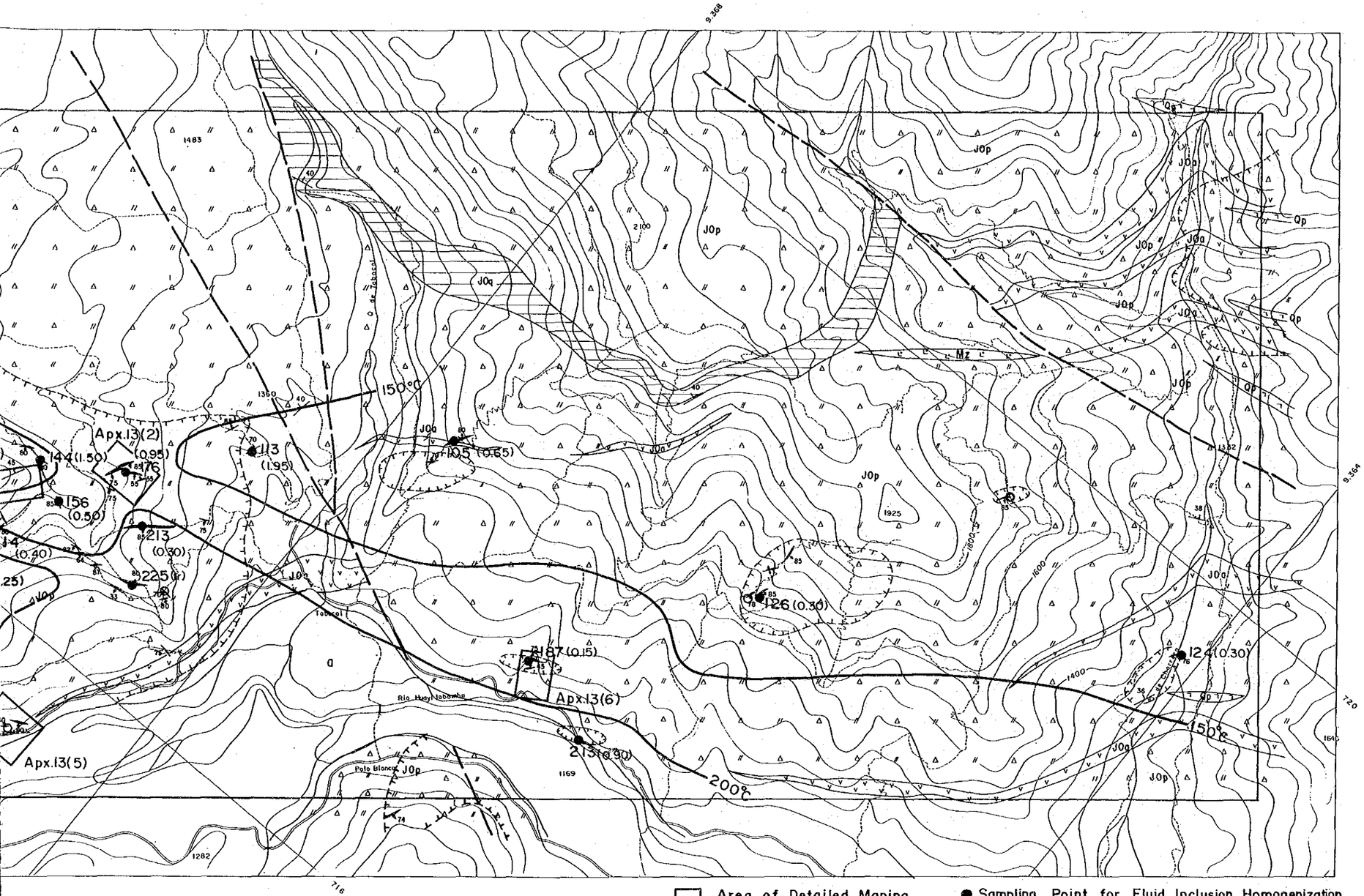

Area of Detailed Maping
See Apx.13 (1) ~ (6)

● Sampling Point for Fluid Inclusion Homogenization Temperature Analysis and Mean of Measured Temperature (°c)

○ Sampling Point of Unavailable Sample, Because of the Absence of Fluid Inclusion

(2.35) Assay Result of Gold in g/t

THE MINERAL EXPLORATION
IN
THE PACHAPIRIANA AREA, REPUBLIC OF PERU
(PHASE II)

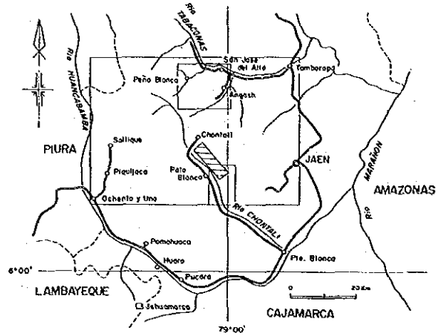

JAPAN INTERNATIONAL COOPERATION AGENCY
METAL MINING AGENCY OF JAPAN
FEBRUARY 1990
Prepared by MINDECO

0 500 1000m

LEGEND

Quaternary	Alluvium		a	Gravel, Sand
Cretaceous	Goyllarisquizga GP.		Kgt	Quartzite
Jurassic	Oyotun Vol.		JOq	Sandstone, Quartzite, Shale
			JOp	Tuff, Lapilli Tuff, Tuff Breccia
Triassic			JOa	Andesite
Intrusives			Mz	Monzonite
			Qp	Quartz Porphyry
Alteration				Silicified and / or Argillized Zone
Others				Quartz Vein
				Fault
				Bedding

Fig. II-6 Distribution of Fluid Inclusion Homogenization Temperature in the Chontali Area

central part of the semi-settled survey area (Fig. Ⅱ-2). They are the area between two major tectonic lines, the area where acidic dykes closely develop and the area along the fault-fissure systems, respectively. Around these alteration zones, argillization or chloritization are commonly developed to suggest the survey area is as a whole an alteration zone in a wide sense. Alteration minerals occurring in the silicified and silicified-argillized zones are analyzed by X-ray diffraction (Apx. 7; A072704, A080502, Y081908, A082401, H082404) to show simple mineral association. The main constituent is quartz and sericite, sometimes associated with a few kaolinite, smectite, jarosite, rutile and anatase.

2) Geochemical survey

In a general view (Table Ⅱ-1), geochemically anomalous zones of gold, silver, lead and copper appear in the detailed survey area and those of gold, silver, zinc and molybdenum in the semi-detailed survey area. Analyzing the distribution of geochemical anomalies per each element (Fig. Ⅱ-4), it is noted that that of gold is large scale overlapping the alteration zones on the northern bank of the Tabacal River as well as small scale overlapping or around the sporadic alteration zones in a small scale. That of silver is small in scale, discontinuous and sporadic. That of lead is also small in scale and discontinuous. Each of geochemically anomalous zone of silver and lead is found in one locality of semi-detailed survey area. That of zinc is small in scale but continuous, and that of copper and molybdenum is small in scale, discontinuous and sporadic. In the detailed survey area the distribution of anomalous zones for gold, silver, lead, zinc and copper overlap each other, but in semi-detailed survey area they hardly overlap.

1-1-5 Results of Chemical Analysis of Ore

Laboratory tests were conducted on 102 samples from the quartz veins developed in the alteration zones in the survey area. The assay results and the distribution of the quartz veins

are shown in Apx. 11 and Apx. 14 (1) to (6), respectively.

The highest graded quartz vein in the area was found in the north of Cruz Pampa, whose width and extension is 2 m and 60 m, respectively, with the grade of 16.15 g/ton Au, 11 g/ton Ag, 50 ppm Cu, 300 ppm Pb, 170 ppm Zn and 8 ppm Mo, having undergone intense Au mineralization. The largest in scale of quartz veins is found as a swarm in Hualatan west (Apx. 14-(1)). This swarm is developed in the area of 200 m × 500 m, constituted by echelon-type six quartz veins, whose average width and extension are 1.45-4.17 m and 40-140m, respectively. They are of high graded Au-Ag mineralization, with the grade of 1.2-7.7 g/ton Au, 11-22 g/ton Ag, 50-250 ppm Cu, 200-578 ppm Pb, 120-210 ppm Zn and 6-43 ppm Mo.

At 1 km south of Tabacal, found is galena-bearing quartz barite vein (Apx. 14-(6)). It is characterized by the occurrence of galena (Max. 2.46 % Pb, Y083102), high grade of Au(2.25 g/ton, V082106) and Ag(47 g/ton, Y083102) and the association with barite(Apx. 6; V082105). Under the microscope, they (V082105, V082106) are composed mainly of galena, with subordinate pyrite, chalcopyrite and secondary minerals of chalcocite and covelline. The analyzed values by homogeneous temperature of fluid inclusions in quartz veins and the distribution of the values are shown in Apx. 5 and Fig Ⅱ-6, respectively. The values for analyzed 30 samples range from 96℃ (Y080808) to 271℃ (A081601), arithmetic means of which is 155℃ . Among the values, those for 17 samples are lower than 150℃ suggesting that the temperature is relatively low.

In a general view for the distribution of the temperature, high temperature area higher than 200℃ is developed in the western lowland and low temperature area lower than 150℃ on the mountains in Hualatan west, Las Pinas and a piedmont in the southern flange of the area. Therefore the distribution is in general that high temperature area is in lower altitude and low temperature area in higher, but at the lowlands of Las Pinas, southern end and of San Francisco, northern end low temperature area lower than 150℃ appears. Taking the distribution pattern of high temperature area into consideration, it is possible to consider that beneath the mountains of Hualatan west there exists

the highest center, say heat source.

1-2 Geophysical Survey

1-2-1 Purpose of the Survey

A purpose of the CSAMT survey is to elucidate resistivity and explore auriferous quartz veins and extension of the mineralization to depths in Chontali area.

1-2-2 Scope of the Survey

The survey area and the transmitting electrode locations are illustrated in Fig. Ⅱ -8.

Scope of the survey is as follows:

Area:	35 km²
Number of station:	102
Number of rock sample:	23

1-2-3 Method of CSAMT Survey

(A flow of the survey is illustrated in Fig. Ⅱ -8.)

1) Principles of CSAMT survey

Controlled Source Audio Frequency Magnetotelluric method (CSAMT method) is a kind of magnetotelluric method with a controlled electromagnetic source. The principles of CSAMT method are based on those of MT method (Magnetotelluric method).

MT method uses natural electromagnetic field as a signal which is generated by electric current flow in ionosphere. On the surface of the ground, one horizontal electric field and one horizontal magnetic field which are orthogonal each other are measured. Electromagnetic field on the surface of the ground is a combination of incident field and secondary induced field. The surface electromagnetic field relates to electrical resistivity of the ground as follows:

$$\rho a = \frac{1}{5f}\left(\frac{Ex}{Hy}\right)^2 \quad \text{----------} \ ①$$

The above equation is given for a homogeneous half-space media where incidental electromagnetic is a vertically-striking plane wave.

ρa : apparent resistivity (Ω m)
f : frequency (Hz)
Ex : electrical field (mV/km)
Hy : magnetic field (gamma)

Skin depth, the following equation, is used as an indicator of exploration depth.

$$\delta = 503\sqrt{\frac{\rho}{f}} \quad \text{----------} \ ②$$

δ : skin depth (m)
ρ : resistivity of media (Ω m)
f : frequency (Hz)

A skin depth is a depth where magnitude of incident electromagnetic field becomes 1/e (= about 37%) of that at the surface of the ground. The above equation says that exploration depth is inverse proportional to a square root of frequency and proportional to a square root of resistivity. Therefore, the lower a frequency of measurement is, the deeper a depth of penetration is.

Natural electromagnetic field is not consistent and always strong enough to make reliable measurement. In order to overcome this deficiency of MT survey. Goldstein and Strangway (1975) suggested to have a grounded wire as a signal source. The general concept of the survey system is as Fig. Ⅱ-9.

As explained above, MT theory is valid only where source electromagnetic field is vertically-impeding and horizontally-polarized. In CSAMT survey, the area where MT theory can be ap-

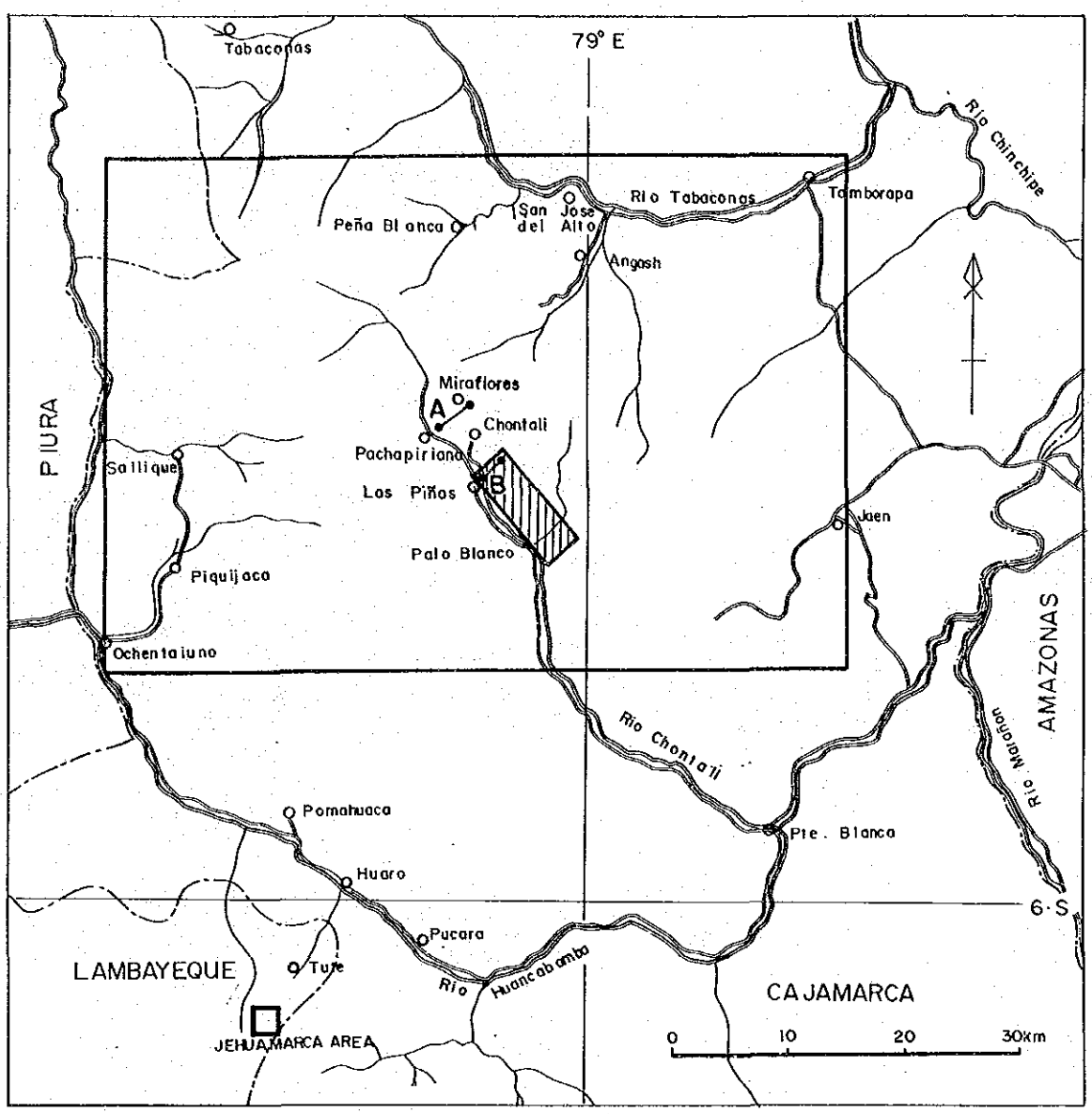

Limits of Department

River

Road

Town and/or Village

Pachapiriana Project Area

Geophysical Survey Area

Transmitter Bipole

Fig. Ⅱ-7 Location of Geophysical Survey Area

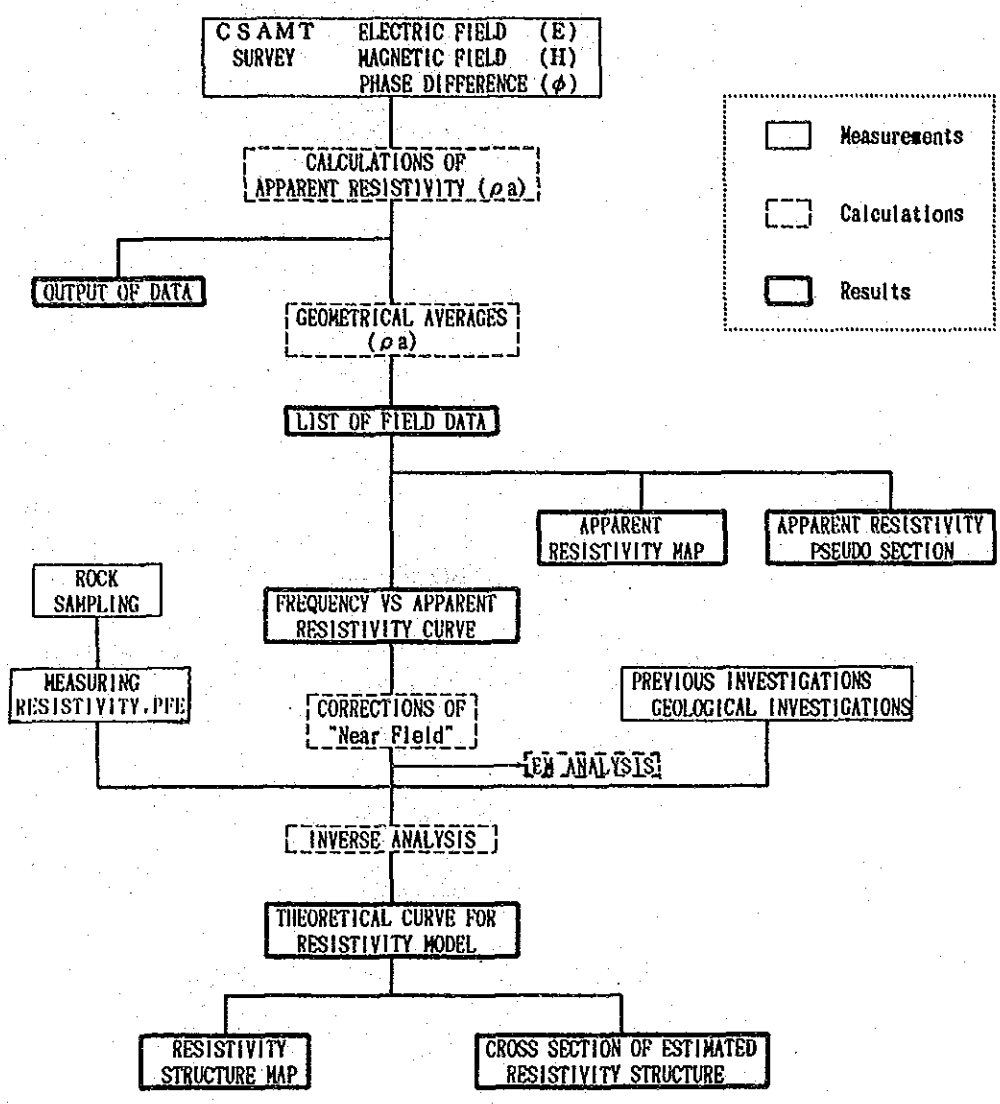

Fig. II－8 Flow Chart for CSAMT Data Processing

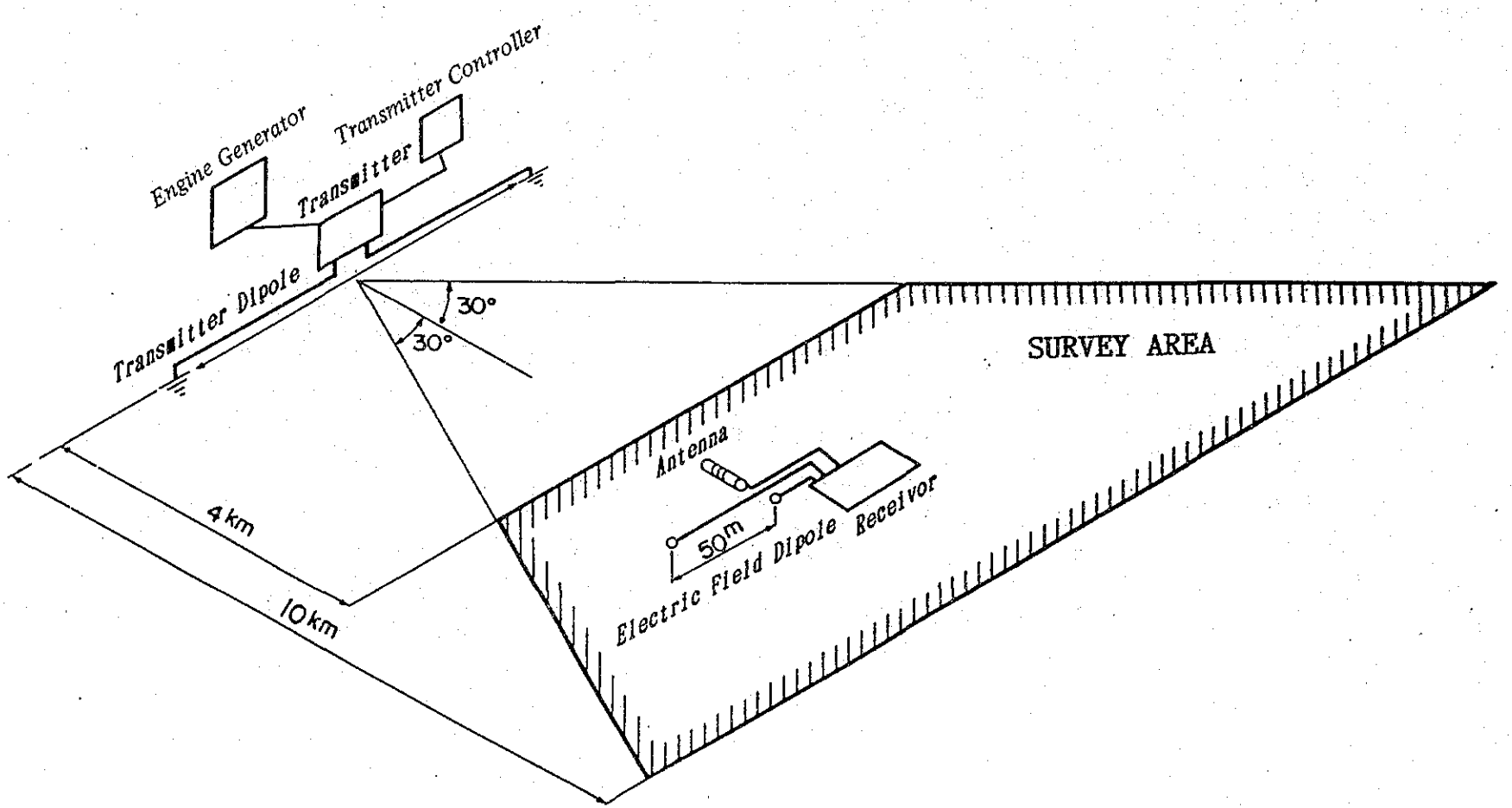

Fig.II—9 Schematic Diagram of CSAMT Survey

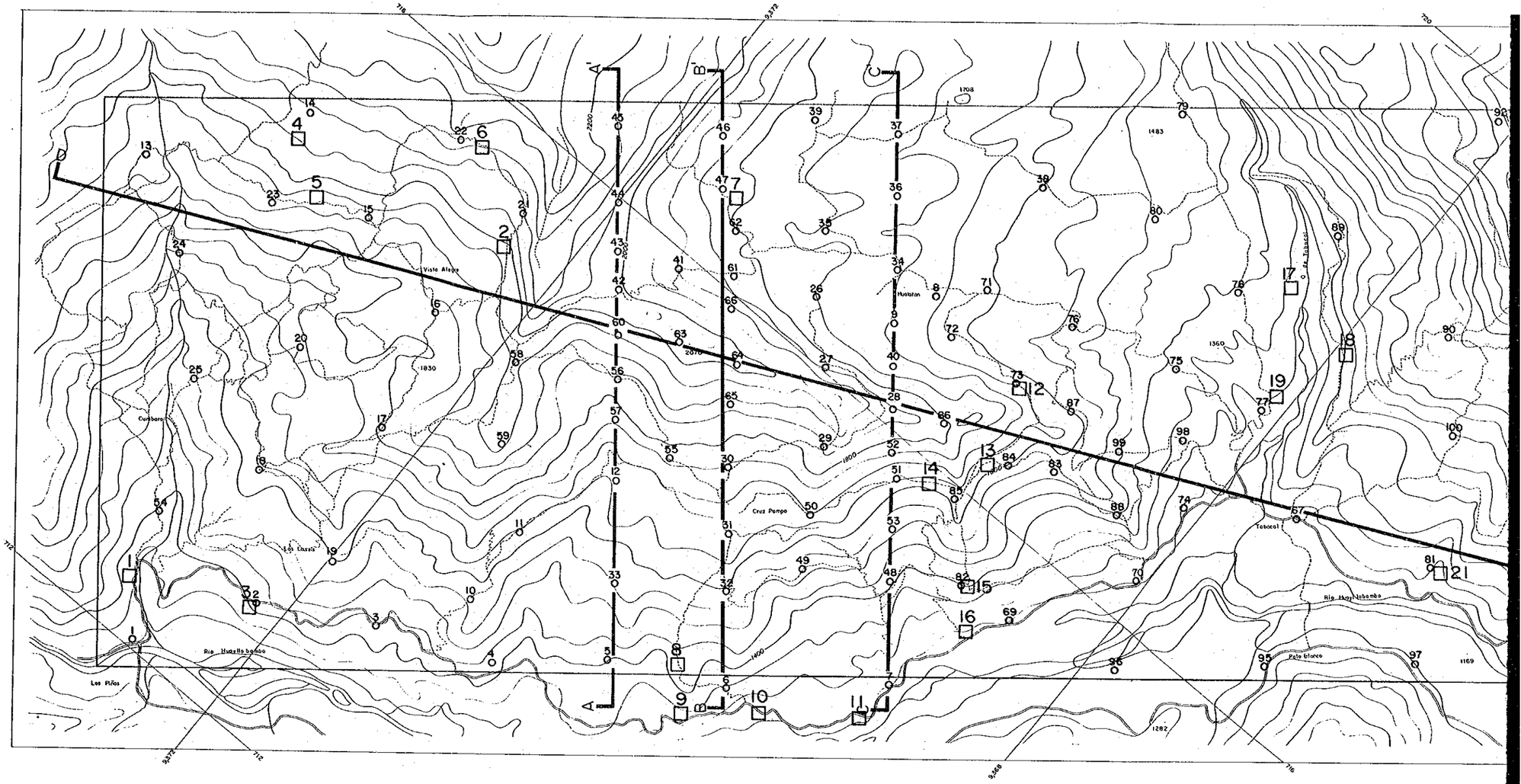

LEGEND

45 Station number
CSAMT Station

A A' Cross Section

1 Sample number

Sampling Station

0 500 1000m

Scale = 1:25,000

Fig.II-10 Location of CSAMT St
and Rock Samples in the Chontali

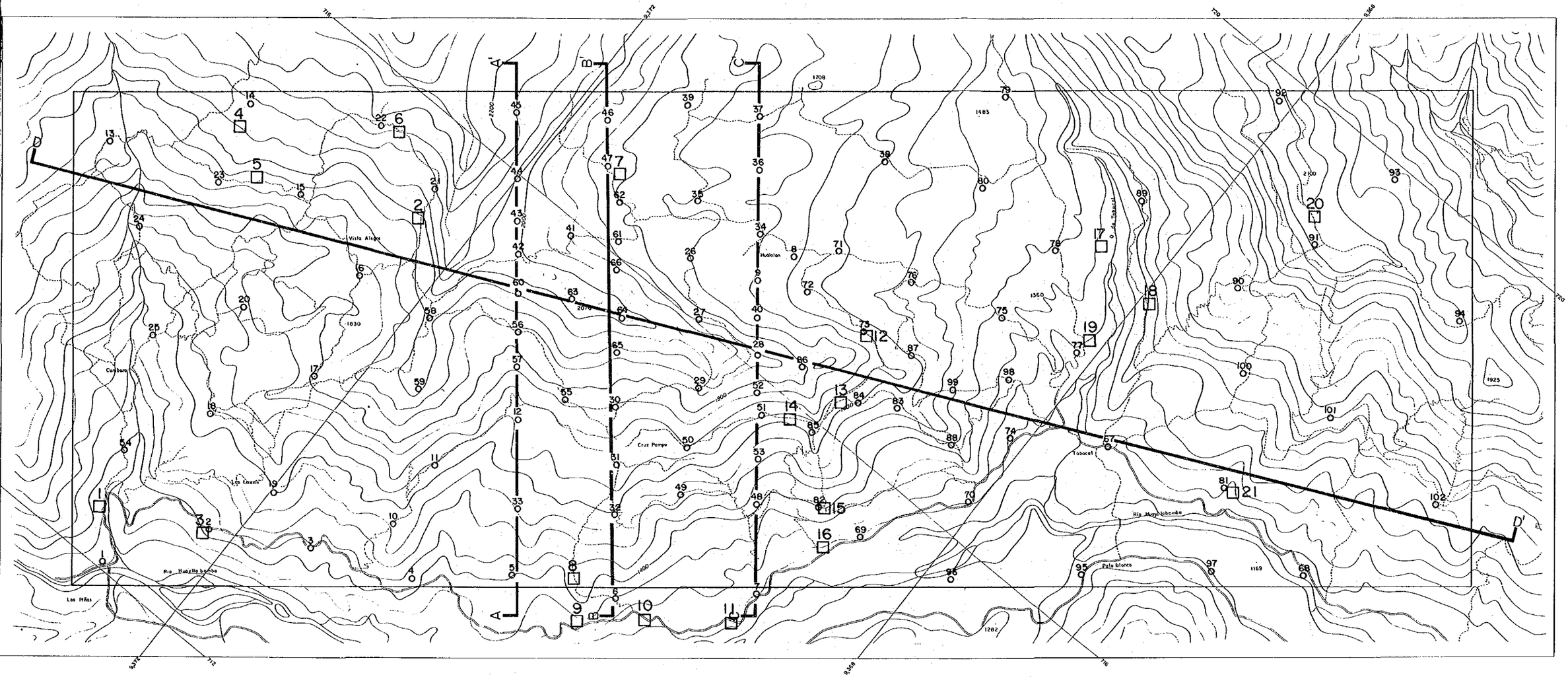

LEGEND

45 Station number
O CSAMT Station

A A' Cross Section

I Sample number

□ Sampling Station

0 500 1000m

Scale = 1:25,000

Fig.II-10 Location of CSAMT Stations and Rock Samples in the Chontali Area

plied must be far away from a source wire, at least three folds of a skindepth, and is called "far field". If a receiving station is closer than three folds of a skindepth from a source cable, apparent resistivity calculated by the equation above does not represent ground resistivity. The area where apparent resistivity does not represent ground resistivity due to too short a distance from a source cable to the station is called "near field".

2) Field Procedure

① Transmitting Cable

Two transmitting cables were used for the survey.

A-bipole: North of the survey area, between Pachapiriana and Miraflores.

B-bipole: Northern part of the survey area, between Las Pinas and the south of Chontali.

Tin plates of 1 m by 2 m are buried 1 m in the ground with mixture of bentonite, salt and water to make contact resistance low. About ten plates are used for one current electrode.

② Stations

Seventy stations are distributed evenly throughout the survey area, about 800 m apart. Around a mineralized zone, stations are densely set along three survey lines, every 200 to 300 m. Locations of stations are marked on the map surveyed by the geological team, 1/5,000 scale.

③ Measurement

At first, signal strength is monitored by an oscilloscope. There are very small electromagnetic noise in the survey area, and data are well repeated. Digital data on a receiver are electric field strength, magnetic field strength, apparent resistivity, and phase difference of electric field and magnetic field. All the data were wrote down on a notebook and judged their validity and repeatability.

Specifications of the used transmitters and receivers are as follows:

④ Signal Source and Receiver

a) Signal source and transmitter:

	A-Bipole	B-Bipole
Length	3,500 m	2,500 m
Direction	N45° E	N45° E
Total resistance	25 Ω	16 Ω
Output current	4 Hz to 128 Hz 12 A	4 Hz to 128 Hz 11 A
	256 Hz to 2,048 Hz 12 to 2.3 A	256 Hz to 2,048 Hz 11 to 3.5 A

b) Receiver:

Receiving dipole direction: TM mode
Distance between station and source: 4 km to 10 km
Receiving dipole length: 50 m
Receiving dipole direction: N45° E (parallel to source bipole)
Magnetic sensor direction: N45° W (orthogonal to source bipole)
Number of repetition at one station: over three times per frequency
Period of measurement: over thirty minutes.

3) Equipment

Equipments used for the survey are made by Zonge Engineering & Research Organization and their specifications are as follows:

① Transmitter

Engine generator(ZMG-7.5):output power 7.5 kVA, 120/208 V, 400 Hz, 3 phase, 18 HP
Transmitter(GGT-6):max. output power 5 kW, max. current 24 A, max. voltage 1,000 V
Transmitter(GGT-20):max. output power 25 kW, max. current 30 A, max. voltage 1,000 V
Transmitter controller(XMT-12):range of control DC to

10,000 Hz

② Receiver

Data processor(GDP-12):amplifier, filter, A/D converter, data processing, frequency range 0.5 Hz to 4,096 Hz

Antenna coil (AMT/1):single axis ferrite coil, sensitivity 0.2 mV/γ Hz

4) TE Mode and TM Mode

There have been used two kinds of source directions for delineating underground geological structure, a source bipole parallel to general strike of geological structure, TE mode, and it perpendicular to a general strike of geological strike, TM mode. Survey results obtained are rather different in TE mode and TM mode. TM mode measurement gives very distinctive anomaly but only over an anomalous body. On the other hand TE mode gives not so distinctive anomaly but wide area. Therefore, for reconnaissance survey, TE mode has been used more widely. However, we used TM mode for this survey due to topographical limitation of the survey area.

General idea of the TE and TM survey results is illustrated below.

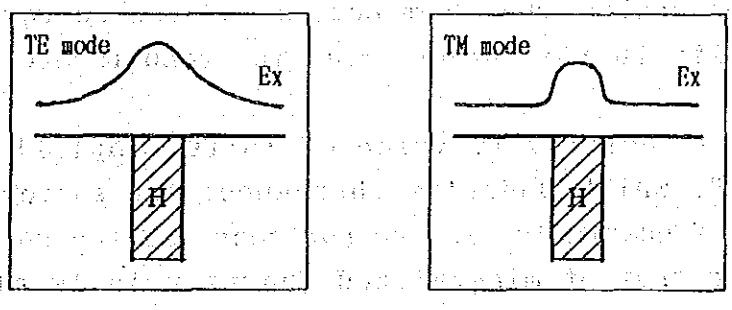

1-2-4 Interpretation

1) Apparent Resistivity

Apparent resistivities were measured at least three times for each frequency at each station. Measured apparent resistivity values were checked and noise contaminated data were discarded. Only good apparent resistivity values were averaged geometrically to get an apparent resistivity for interpretation at each frequency of each station.

Average apparent resistivity values are tabulated in Table Ⅱ-2.

2) One Dimensional Inversion

Because MT theory cannot be used for CSAMT data collected in "near field" zone, many people suggested simple near field correction for those near field contaminated data. However, no simple near field correction can remove near field effect from data so that we used direct one dimensional inversion method taking source bipole in consideration. The computer program used is called "CSINV" of which forward model calculation is by Wait (1961). All the results are shown in Appendix 16.

1-2-5 Results of the Survey

1) Laboratory Sample Measurement

Resistivity and PFE are measured on 23 rock samples of which 21 samples are collected in the survey area and two samples, granodiorite and schist, are from outside of the survey area assumed to underlie in the survey area. The results are tabulated in Table Ⅱ-3.

The average resistivity value of tuffs, lapilli tuff and silicified tuff, which underlie throughout the survey area, is 530 Ω m. That of quartzite, in the northeast of the survey area, is 3,900 Ω m and that of mineralized quartz vein is also high, 2,900 Ω m. Therefore we assume that strongly silicified zones where quartzite and quartz veins are can be delineated as a resistive zone. Even though number of samples only two, resis-

Table Ⅱ—2 List of Apparent Resistivity

ST.NO. & DIPOLE	FREQUENCIES (Hz)									
	4	8	16	32	64	128	256	512	1024	2048
1	3730	1930	1000	475	167	36	71	66	60	42
2	5460	2960	1520	700	238	214	255	191	174	261
3	1470	835	468	226	79	47	71	53	46	42
4	682	528	385	217	66	11	33	29	26	22
5	548	318	184	89	24	20	21	17	16	16
6	3250	1820	960	423	105	116	112	77	95	79
7	628	337	159	60	18	36	29	29	29	42
8	804	383	147	72	110	124	111	104	84	105
9	727	342	127	69	122	115	124	94	84	59
10	1130	603	268	105	36	47	52	56	100	171
11	246	126	60	23	17	30	30	34	44	50
12	524	277	139	54	36	63	54	35	47	38
13	451	238	134	77	68	86	85	77	69	61
14	11	6	3	3	5	8	12	15	22	12
15	634	350	189	105	127	127	152	197	235	281
16	81	42	18	12	20	20	21	24	30	46
17	414	222	115	53	50	73	74	49	78	156
18	571	284	134	56	23	36	42	37	34	17
19	3350	1870	1010	482	175	172	205	172	216	54
20	648	342	169	77	49	82	75	63	55	55
21	431	213	92	72	116	123	144	154	180	173
22	494	244	100	74	98	81	71	63	42	133
23	820	436	217	123	192	254	298	337	346	323
24	266	143	74	35	21	37	43	45	44	42
25	992	543	288	138	54	39	59	55	61	63
26	326	163	69	33	55	64	63	59	54	53
27	1780	810	309	152	265	345	330	314	245	189
28	991	421	150	112	209	238	204	236	348	517
29	592	294	111	57	149	182	216	405	956	3520
30	876	441	200	93	144	190	161	135	104	83
31	250	118	51	18	25	41	48	111	186	902
32	1490	815	359	149	47	92	58	150	497	2380
33	2970	1490	664	249	98	150	112	160	772	2340
34	265	121	51	40	67	78	82	70	110	222
35	343	177	73	42	72	88	83	108	339	132
36	311	144	57	42	70	83	97	101	117	119
37	292	139	53	38	61	64	69	61	51	40
38	440	202	81	23	49	49	46	42	37	33
39	291	126	49	52	95	199	335	1270	6260	5870
40	1670	783	305	157	265	293	251	217	191	126
41	220	117	51	37	66	83	95	100	115	115
42	182	71	26	45	82	99	242	144	167	384
43	670	307	131	91	155	180	180	200	203	209
44	2650	1540	628	455	704	835	994	1010	1040	1030
45	732	378	157	128	212	200	258	273	309	486
46	444	213	88	45	80	105	132	494	2110	3610
47	824	262	106	84	156	180	213	138	255	151
48	3430	1770	806	284	126	243	204	170	141	183
49	1480	760	365	124	59	116	112	114	99	51
50	805	386	171	57	56	101	88	77	66	424
51	1420	692	297	146	126	201	182	203	204	240
52	1150	542	217	86	155	221	201	205	215	247

(Ω·m)

Table Ⅱ−2 List of Apparent Resistivity

ST.NO. & DIPOLE	FREQUENCIES (Hz)									
	4	8	16	32	64	128	256	512	1024	2048
53	1210	627	289	89	54	106	96	81	80	60
54	3920	2190	1190	600	240	58	139	114	101	83
55	1070	529	245	106	166	242	245	176	124	823
56	687	351	159	83	155	202	206	232	209	247
57	290	153	76	34	52	71	68	77	79	125
58	85	43	22	20	43	52	55	64	242	334
59	51	27	14	8	12	19	21	22	24	12
60	253	109	47	32	68	77	97	56	11	446
61	204	105	44	35	63	82	87	98	160	16
62	655	310	121	84	156	182	198	182	170	124
63	234	118	60	37	69	106	145	162	259	525
64	289	162	83	45	85	123	172	81	243	891
65	219	104	45	39	71	94	116	121	158	327
66	3180	1480	618	490	892	1060	1080	1060	887	185
67	1920	815	281	65	58	69	68	55	47	40
68	3390	1820	822	235	80	131	87	52	33	21
69	5450	2520	1090	397	140	198	189	155	136	120
70	420	199	92	33	12	22	16	14	16	19
71	1870	881	392	131	170	216	202	178	147	190
72	900	460	219	77	77	103	86	72	61	50
73	2740	1190	445	133	173	269	226	191	185	870
74	456	230	115	41	16	25	17	13	12	5
75	572	268	106	25	33	36	29	28	37	63
76	338	190	98	34	31	40	35	38	40	47
77	1170	502	180	34	47	58	56	46	43	26
78	644	268	89	17	46	38	32	26	25	24
79	328	143	48	13	37	31	29	27	26	30
80	467	209	82	20	39	34	29	27	26	28
81	5280	1980	692	126	139	185	129	108	100	77
82	3700	1760	793	299	104	161	171	162	156	175
83	699	392	226	96	53	87	86	86	87	101
84	1270	558	221	66	62	103	99	104	103	90
85	3680	1920	994	422	218	396	429	481	550	667
86	147	56	16	4	9	15	17	22	29	32
87	1820	1080	606	249	174	263	258	273	279	262
88	2770	1260	559	191	118	218	199	208	234	120
89	1980	906	318	62	180	175	177	205	216	292
90	103	49	15	7	20	19	21	41	41	56
91	510	217	77	75	158	172	191	199	278	72
92	993	334	108	208	366	421	448	566	657	527
93	224	96	26	41	82	74	100	150	348	24
94	441	167	67	37	75	82	88	77	80	127
95	5260	2340	945	278	98	160	90	68	57	41
96	3740	2110	1140	475	105	173	124	93	77	54
97	1860	980	452	139	53	87	46	34	28	24
98	2090	1020	460	138	87	116	76	56	42	33
99	4710	2110	817	237	163	261	212	210	179	204
100	258	120	42	11	27	26	24	28	37	32
101	671	357	146	38	56	53	52	50	54	60
102	1960	941	370	91	94	85	62	56	50	54

(Ω·m)

No.	Rock name	Location	Silicification	Chloritization	Argillization	Resistivity (Ω・m)		PFE (%)	
15	andesite (g. t. b.)	Tabacal	○			4, 100		0. 8	
2	〃	Vista Alegre		○		1, 200	2, 300	1. 6	1. 2
18	〃	Tabacal		△		1, 500		1. 1	
5	tuff breccia	Vista Alegre		○		390		2. 7	
21	〃	Tabacal		○		870		2. 0	
9	〃	Tabacal		○		400		1. 5	
11	〃	Tabacal	○		○	860	530	3. 3	2. 5
3	lapilli tuff	Los Laureles	○			410		2. 9	
14	〃	Hualatan	△			190		3. 0	
8	silicified tuff	Tabacal	◎			670		1. 9	
10	〃	Tabacal	◎			420		2. 3	
13	quartz-vein	Hualatan	○			4, 000	2, 900	2. 1	2. 0
1	〃	Las Pinas				1, 700		2. 0	
16	quartzite (r. s.)	Tabacal				4, 900		1. 1	
6	〃	Vista Alegre				3, 600		2. 5	
4	〃	Vista Alegre				3, 900	3, 900	0. 6	1. 3
7	〃	Hualatan				4, 600		1. 2	
20	〃	Tabacal				2, 300		1. 3	
12	silicified rock	Hualatan	◎			1, 800		3. 3	
17	marl (r. s.)	Tabacal				260	420	2. 3	1. 9
19	〃	Tabacal				580		1. 5	
	granodiorite	Palo Blanco				1, 000		2. 3	
	schist	Calabozo				180		3. 1	
						MEAN	1, 700		2. 0

remark : g. t. b. : grain of tuff breccia, r. s. : rolling stone

◎very strong , ○strong, △weak

Table Ⅱ－3 Result of Rock Properties

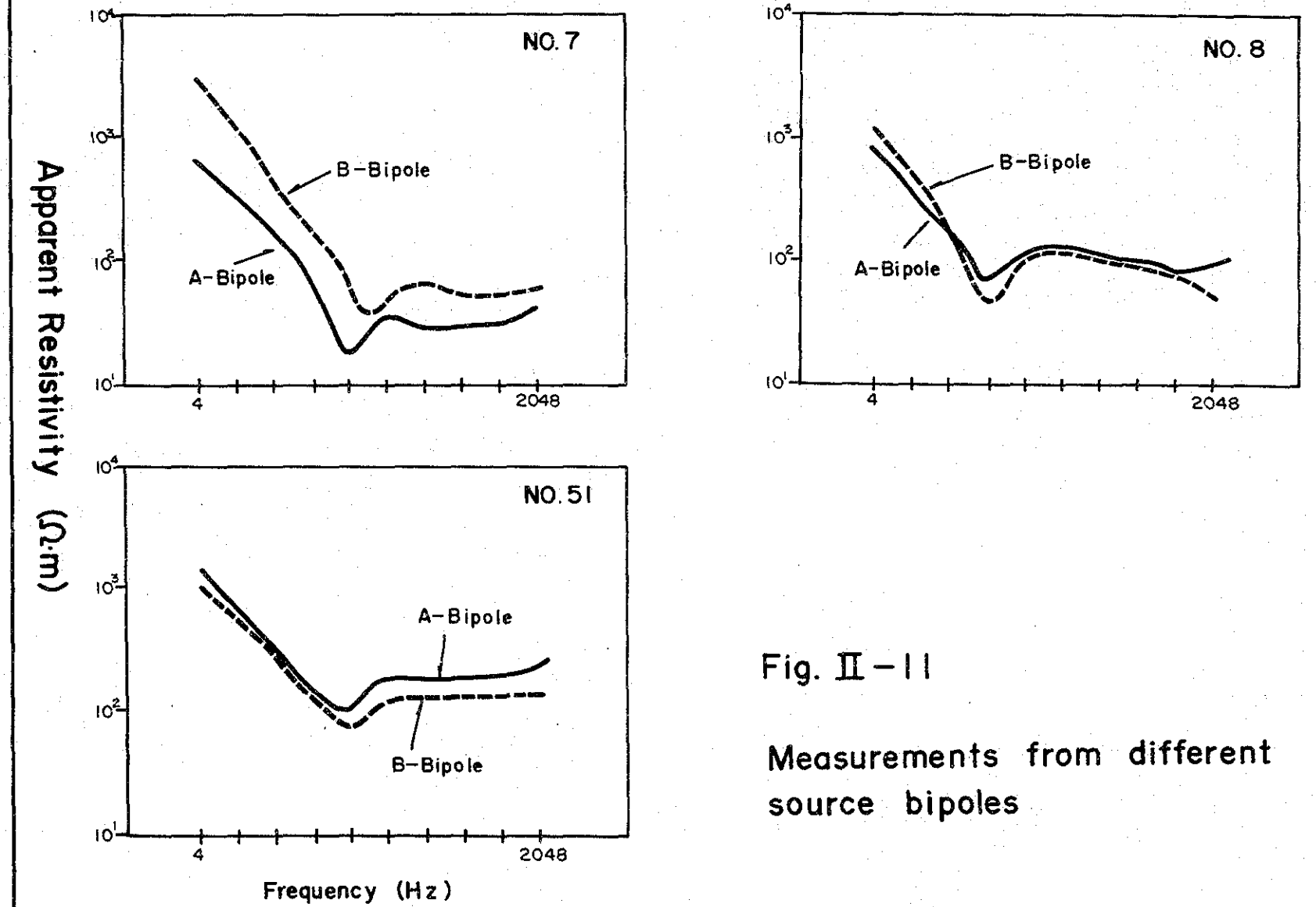

Fig. II-11

Measurements from different source bipoles

tivities of granodiorite, 1,000 Ω m, and schist, 180 Ω m, show significant difference. Most silicified rock shows high resistivity but it also depends on samples.

The average value of all rock samples is relatively low, 3.3 %. It shows that rock samples do not contain large amount of polarizable minerals, like sulfide mineral. Because all rock samples are collected from the surface of the ground and sulfide mineral may altered by weathering, PFE of rocks in the ground may not be so low.

2) Survey Result

① Comparison of Measurements by Two bipoles, A-bipole and B-bipole

We made measurement repeated at three stations, No. 7, 8, and 51 by using two different signal sources, A-bipole and B-bipole. The results are shown in Fig. Ⅱ-11. The results show that the repeated measurements by two different sources are very similar and no systematic shift of the data is recognized. For the three stations A-bipole is further from stations and less near field effect is expected so that data by A-bipole are used for interpretation.

② ρ a-f Spectrum Map

Apparent resistivity values at each stations are plotted against frequency, which is called ρ a-f spectrum. ρ a-f spectrum at each station are illustrated on ρ a-f spectrum map, PL.-8, at location of each station. All spectra show steep rising of apparent resistivity in lower frequency between 32 Hz and 4 Hz which is typical for near field effect and under-shoot between 32 Hz and 64 Hz typical in transition zone. Therefore, resistive layer is inferred in depths throughout the survey area. ρ a-f spectra are categorized into the following four types.

LU and LD type, straight between 2,048 Hz and 64 or 128 Hz.

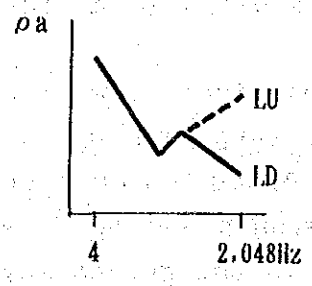

LU type: a becomes high in high frequency.

LD type: a becomes low in high frequency.

CU and CD type, curve between 2,048 Hz and 64 or 128 Hz.

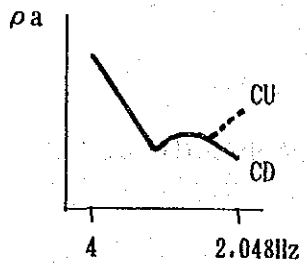

CU type: a becomes high in high frequency.

CD type: a becomes low in high frequency.

Resistivity structures in the ground are assumed to be as follows:

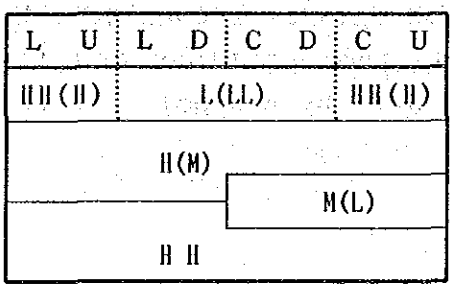

where, HH: very resistive medium
H: resistive medium
M: moderate medium
L: conductive medium
LL: very conductive medium

LU type spectrum shows three layer earth, HH (H) - H (M) - HH. LU type spectrum is around Vista Alegre in the northern part of the survey area and in the southern and central part of the survey area.

LD type spectrum represents three layer earth, L (LL) - H (M) - HH. It is along Rio Huayllabamba and Tabacal in the southern part extending N45° E and north.

CD type spectrum shows four layer earth, L (LL) - H (M) - M (L) - HH. There are only 13 stations with CD type spectrum in the northern part extending N-S direction around Hualantan.

CU type spectrum represents four layer earth, HH (H) - H (M)

- M (L) - HH. It is wide spread around Los Laureles, Cruz Pampa and Hualatan. Apparent resistivity of 2,048 Hz is largely differ from that of 1,024Hz at ten stations, Nos. 29, 31, 32, 33, 39, 46, 50, 55, 60, and 64. Those data are contaminated by geological or some other noise and are interpreted without using apparent resistivity of 2,048 Hz.

Mineralized zone are contact of CD type zone and CU type zone. We assume conductive zone is between CD type zone and CU type zone.

③ Apparent Resistivity Map

Horizontal distributions of apparent resistivity at each frequency show similar trend. Here apparent resistivity maps of 2,048 Hz, 256 Hz, 64 Hz and 4 Hz are explained. Because at the center of the survey area, there are stations densely distributed and mineralized zones, apparent resistivity distribution is complicated.

a) Apparent resistivity map of 2,048 Hz
(Fig. Ⅱ-12(1) and PL.Ⅱ-9(1))

High apparent resistivity zone, over 200 Ω m, is around Cruz Pampa and the southeast of Vista Alegre in the west of Hualatan at the center of the survey area and apparent resistivity value at its center is as high as 2,000 Ω m. There are also resistive zones in the north of Vista Alegre and in the southeastern part of the survey area. Major mineralized zones in the survey area are in the west of Hualatan extending N-S direction and a high apparent resistivity zone runs along with it. A weak low apparent resistivity zone parallel runs due east of the resistive zone. The high apparent resistivity zone around Cruz Pampa is at where an alteration zone is. The high resistivity zone in the southeast of Vista Alegre is located as if an extension of the resistivity zone around Vista Alegre. However, the high resistivity zone in the southeast of Vista Alegre is not caused by mineralization like others but caused by quartzite distribution. Low apparent resistivity zones, under 50 Ω m, are in the northern part of the

survey area, centered by stations No. 18 and 50, correspond to distribution of Monzonite. A low apparent resistivity, under 50 Ω m, belt extends in N45° E direction from Palo Blanco to Tabacal in the south of the survey area. Its location and direction coincide with those of an inferred fault. Thus the apparent resistivity map is concordant with geology of the area.

b) Apparent resistivity map of 256 Hz
(Fig. Ⅱ -12(2) and PL. Ⅱ -9(2))

The high apparent resistivity zone in the center of the survey area, which also seen in the map of 2,048 Hz, becomes small in the area but still extends in the same direction, north-south. The resistive zone corresponds to mineralized zone more obvious than in 2,048 Hz. The resistivity zone in the west of Cruz Pampa of 2,048 Hz disappears in this map, 256 Hz which implies a resistive body caused this high apparent resistivity zone does not extend to depths. Apparent resistivity value at the station No. 86 is low, 20 Hz and forms a low apparent resistivity zone as 2,048 Hz. However, the low apparent resistivity zone of 2,048 Hz extending from the station No. 86 to the west of Hualatan disappears on the map of 256 Hz. A low apparent resistivity strip, under 50 Ω m, extends to southwest direction from Vista Alegre in the north of the survey area and is expansion of the low apparent resistivity zone around the station No. 59 in 2,048 Hz.

c) Apparent resistivity map of 64 Hz
(Fig. Ⅱ -12(3) and PL. Ⅱ -9(3))

Apparent resistivity distribution of 64 Hz is similar to it of 256 Hz. The high apparent resistivity zone at the center of the survey area extends north-south direction, from the station No. 66 to No. 28, with smaller size coinciding with mineralized zone. The high apparent resistivity zone at the northeast of Vista Alegre shrinks its size with depth, so it implies that quartzite does not extends in depths. Generally, low apparent zones becomes larger than those of 256 Hz. The low apparent resistivity zone, under 50 Ω m, in west of Vista Alegre in the

northern part of the survey area is large and extends to the south end of the survey area. However, because the transmitting bipoles are at the north side of the survey area and distance from survey station to the bipoles is closer at the northern part of the survey area than at the southern part, apparent resistivity under-shoot at "transition zone" may cause low apparent resistivity zone in the northern part of the survey area.

d) Apparent resistivity map of 4 Hz
(Fig. Ⅱ-12(4) and PL.Ⅱ-9(4))

Most of the survey area is covered by high apparent resistivity area over 200 Ω m. This high apparent resistivity is caused by "near field effect, but it tells that the survey area is underlain by a resistive basement. Mineralized zone corresponds to the very high apparent resistivity zone over 1,000 Ω m. Apparent resistivity is higher toward the west and it shows that a resistive basement is shallow toward west. There are some lower apparent resistivity zones, under 100 Ω m in the west of Vista Alegre.

④ Apparent Resistivity Pseudosection
(Fig. Ⅱ-12(1), (2), (3), (4) and PL.-10(1), (2), (3), (4))

Three apparent resistivity pseudosections, A-A', B-B' and C-C', crossing a mineralized zone extending N-S direction at the center of the survey area and one apparent resistivity pseudosection, D-D', parallel to the mineralized zone are drawn. All the pseudosections show higher apparent resistivity in lower frequency because of "near field effect" contamination. However, "near field effect" contamination in lower frequency data implies resistive basement in depths. Apparent resistivity of intermediate frequencies is mostly low because of conductive layer over the resistive basement, even though some may be caused by under-shoot. That of higher frequency is mostly high and it implies resistive layer at near the ground surface. At the center of the pseudosections, resistivity contours are vertical and it implies lateral discontinuity of resistivity structure there.

The apparent resistivity pseudosections between No. 12 and No. 42 of the section A-A', between No.32 and No. 64 of the section B-B', and between No. 28 and No. 53 of the section C-C' are very similar shape of resistivity contours, so the three parts of each section are as if having a continuous structure. A high apparent resistivity over 200 Ω m vein intrudes at the station No. 66 of the section B-B'. At the stations No. 28, No. 32 and No. 64 of the section B-B', there found high apparent resistivity in higher frequency which coincide with mineralized zone.

Along the section D-D', between No. 58 and No.64, a higher apparent resistivity changes a lower apparent resistivity in lower frequency, are as if having a continuous structure. No. 16, No. 86 and No.74 are under 100 Ω m in every frequency.

3) Result of Interpretation

Apparent resistivity data at all stations are one dimensionally inverted by the computer program with source bipole in consideration.The inverted results are tabulated in Appendix. Interpreted results are as expected from ρ a-f spectrum classification. Results are illustrated as four resistivity sections, A-A' to D-D', two resistivity structure maps, +1,600m and +1,200m, and a three-dimensional resistivity map.

① Resistivity Structure Section
(Fig. Ⅱ-12(1), (2), (3), (4) and PL.-10(1), (2), (3), (4))

The results of one dimensional interpretation give the bottom layer resistivity of between 500 Ω m and 1,000 Ω m. We assumed it a resistive basement of the area.

Undulation of the resistive basement is large for the three sections, A-A', B-B' and C-C'. The basement upheaves at the central part of the three sections, between the stations No. 42 and No. 56 of the section A-A', between the stations No. 65 and No. 66 of the section B-B', and at the station No. 40 of the section C-C'. Upheaved parts of the basement are mostly covered with conductive layer under 100 Ω m, even some part being under 50 Ω m. Around those upheaved parts of the basement resistivity struc-

A
A'
B
B'
C
C'
D
D'
HH
LL
H
L
Vista Alegre
Cumbaro
Los Llanos
Cruz Pampa
Tobacal
Río Hondo
Río Negro
Palo blanco
Los Pilas

THE MINERAL EXPLORATION
IN
THE PACHAPIRIANA AREA, REPUBLIC OF PERU
(PHASE II)

Fig. II-12 (1) Apparent Resistivity Map of the Chontali Area (2,048 Hz)

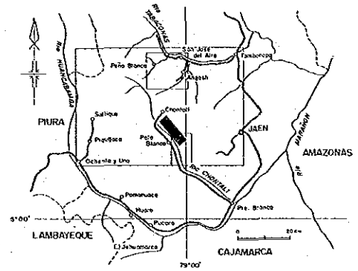

JAPAN INTERNATIONAL COOPERATION AGENCY
METAL MINING AGENCY OF JAPAN
FEBRUARY 1990
Prepared by MINDECO

LEGEND

45 Station number
O CSAMT Station
202 Apparent Resistivity (Ω-m)
A A' Cross Section

Division of Apparent Resistivity
20 50 200 500 (Ω-m)
LL | L | H | HH

10 Apparent
20 Resistivity
50 Contour (Ω-m)

0 500 1000m
Scale = 1 : 10,000

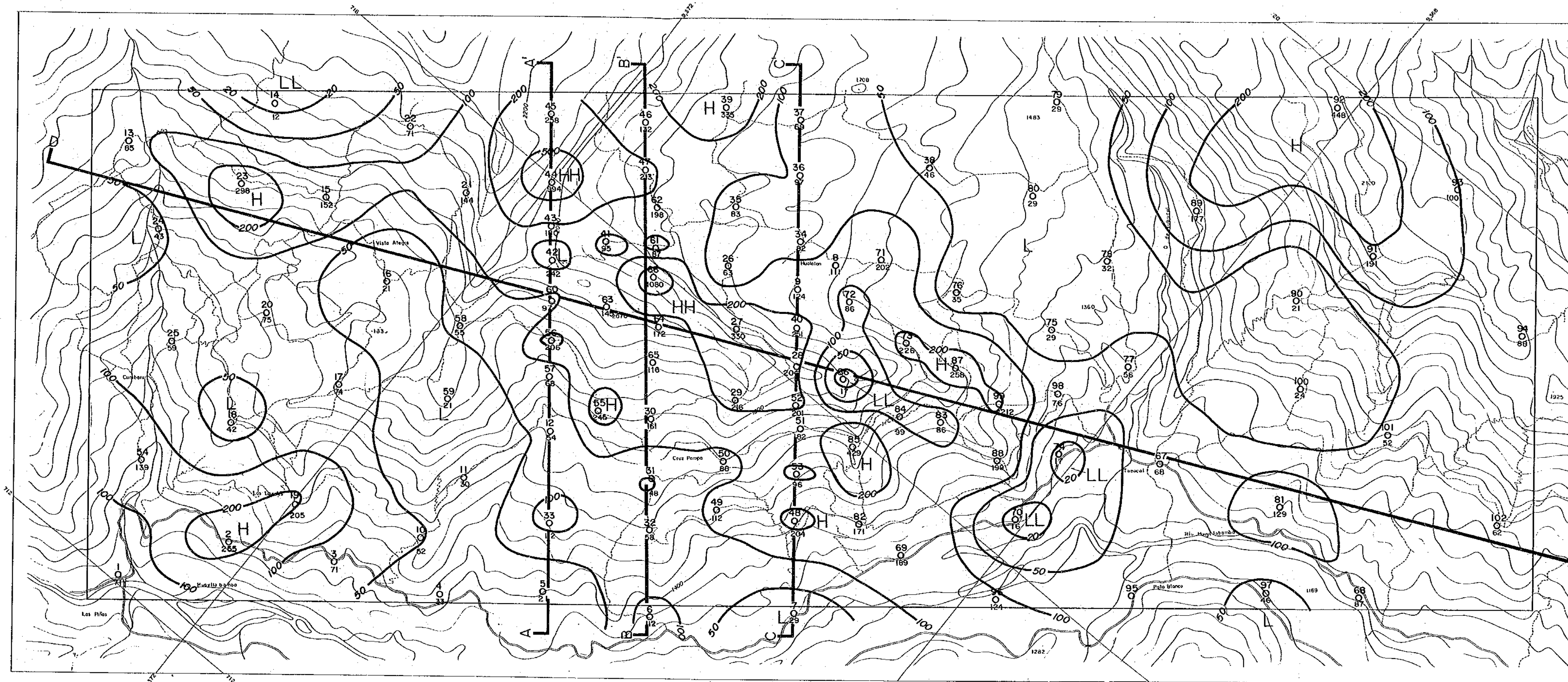
A
A'
B
B'
C
C'
D
Vista Alegre
Cruz Pampa

THE MINERAL EXPLORATION
IN
THE PACHAPIRIANA AREA, REPUBLIC OF PERU
(PHASE II)

Fig. II-12(2) Apparent Resistivity Map of the Chontali Area (256 Hz)

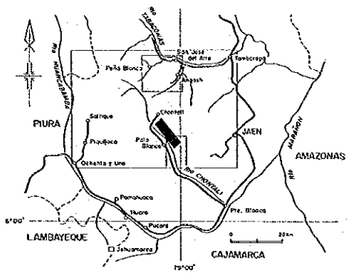

JAPAN INTERNATIONAL COOPERATION AGENCY
METAL MINING AGENCY OF JAPAN
FEBRUARY 1990
Prepared by MINDECO

LEGEND

45 Station number
CSAMT Station
202 Apparent Resistivity (Ω-m)

A A' Cross Section

Division of Apparent Resistivity
20 50 200 500 (Ω-m)
LL | L | H | HH

10 Apparent Resistivity Contour (Ω-m)
50 Contour (Ω-m)

0 500 1000m
Scale = 1 : 10,000

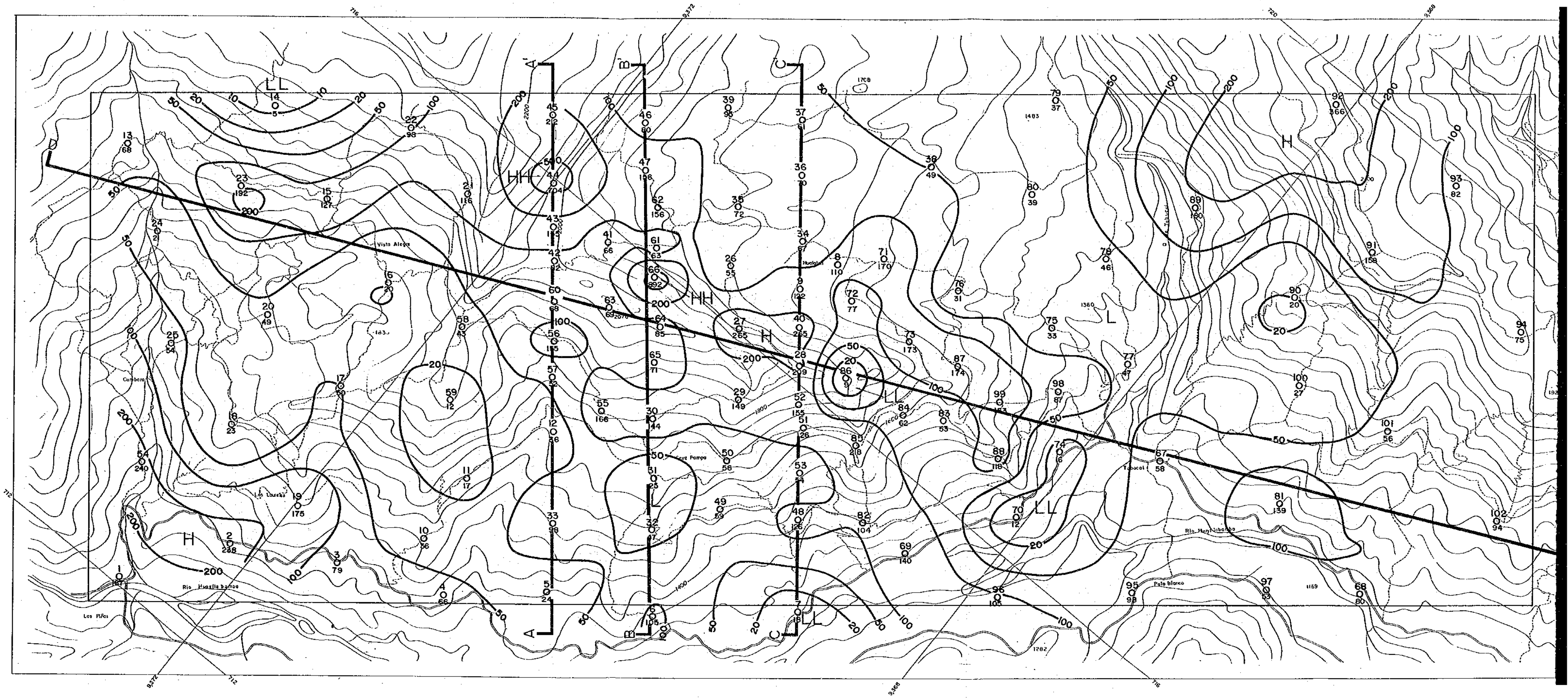

A
A'
B
B'
C
C'
D
HH
H
LL
L

THE MINERAL EXPLORATION
IN
THE PACHAPIRIANA AREA, REPUBLIC OF PERU
(PHASE II)

Fig. II-12(3) Apparent Resistivity Map of the Chontali Area (64Hz)

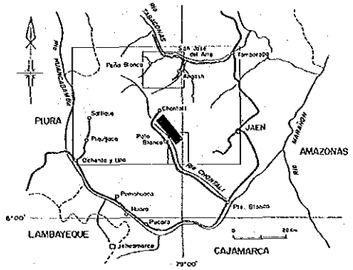

JAPAN INTERNATIONAL COOPERATION AGENCY
METAL MINING AGENCY OF JAPAN
FEBRUARY 1990

Prepared by MINDECO

LEGEND

- 45 Station number
- CSAMT Station
- 202 Apparent Resistivity (Ω-m)
- A A' Cross Section

Division of Apparent Resistivity

20	50	200	500 (Ω-m)
LL	L	H	HH

- 10 Apparent
- 20 Resistivity
- 50 Contour (Ω-m)

0 500 1000m

Scale = 1 : 10,000